Solids containing Si-O-P bonds: is the hydrolytic sol-gel route a suitable synthesis strategy?

Journal of Sol-Gel Science and Technology
https://doi.org/10.1007/s10971-023-06241-4

ORIGINAL PAPER

Solids containing Si-O-P bonds: is the hydrolytic sol-gel route a suitable synthesis strategy?

Claudio Imparato[1] · Aurelio Bifulco[1] · Giulio Malucelli[2] · Antonio Aronne[1]

Received: 25 May 2023 / Accepted: 3 October 2023

Abstract

Materials based on silicon-phosphorus mixed oxides have traditionally attracted interest in electronics, optics, catalysis, and related fields. The preparation of a solid containing stable Si–O–P linkages is a huge challenge due to their intrinsic instability to hydrolysis in a wet atmosphere. On the other hand, most technological applications of these materials, such as protonic conductive membranes in fuel cells and water-tolerant solid acid catalysts, are related to their interaction with water; consequently, suitable synthesis procedures that positively face this tradeoff are mandatory. Besides the traditional high-temperature techniques, sol-gel synthetic methods represent a viable, low-cost alternative, allowing for the preparation of high-purity materials with a homogeneous distribution of the components at the atomic scale. Si–O–P linkages are easily obtained by nonhydrolytic sol-gel routes, but only in inert and dry atmosphere. Conversely, hydrolytic routes offer opportunities to control the structure of the products in a wide range of processing conditions. The present review aims at providing an overall picture of the research on the sol-gel synthesis of phosphosilicate and related materials and theisr different applications, emphasizing how the interest in these systems is still lively, considering both conventional and emerging applications, such as flame retardance. The incorporation of Si–O–P nanostructures in polymer composites, coatings, and textiles is indeed a promising strategy to improve properties like thermal stability and fire resistance; however, their in-situ synthesis brings about additional difficulties related to the reactivity of the precursors. The perspectives linked with the development of Si–P-based materials are finally outlined.

Graphical Abstract

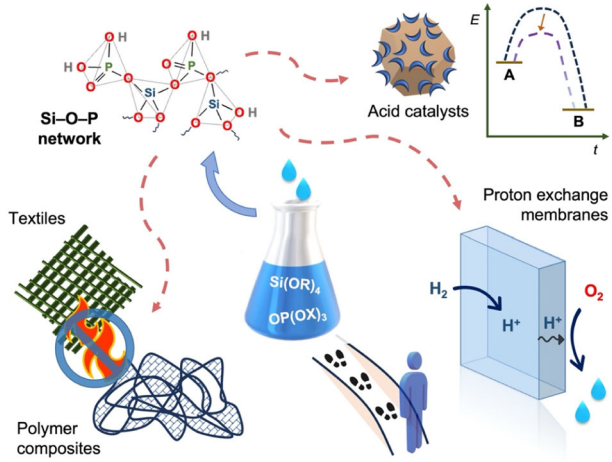

✉ Antonio Aronne
antonio.aronne@unina.it

[1] Department of Chemical, Materials and Production Engineering (DICMaPI), University of Naples Federico II, Piazzale Tecchio 80, 80125 Napoli, Italy

[2] Department of Applied Science and Technology, Politecnico di Torino, and local INSTM Unit, Viale Teresa Michel 5, 15121 Alessandria, Italy

Published online: 14 October 2023

Keywords Hydrolytic sol-gel processes · Si-O-P nanostructures · Si-P oxides · Phosphosilicate · Flame retardance

Highlights

- Si–O–P linkages show an intrinsic low stability to hydrolysis.
- Hydrolytic sol-gel processing in suitable conditions can produce extended Si–P cross-condensation.
- The introduction of a metal in the phosphosilicate network can stabilize P and prevent its leaching.
- The formation of Si–P nanostructures can be favored in a polymer matrix, giving hybrid composites.
- Si–P oxides have interesting application prospects in fuel cells, acid catalysis, flame retardance.

1 Introduction

Silicon-phosphorus mixed oxides (SiO_2-P_2O_5) have distinctive physical and chemical properties, such as ionic exchange and electrical conductivities, surface acidity, high dimensional stability, and porous structure. Thus, they are important in a variety of application fields, particularly in electrochemical systems as proton-conducting membranes, in optoelectronic and photonic devices as waveguides or host matrices, in catalysis as solid acids, in the manufacturing of polymers, composites, and textiles as flame retardants, and in biomaterials as porous scaffolds for bone tissue engineering.

The Si-P binary oxide system has been studied for more than a century, with several works dealing with the structure and composition of the materials [1]. However, most currently relevant applications have been investigated only during the last two or three decades. In the development of power sources relying on hydrogen or other sustainable fuels, proton exchange membrane (PEMs) fuel cells play a key role [2]. Phosphosilicate gels and glasses are promising candidates for the manufacturing of efficient and stable PEMs because of their high proton conduction ability and proper thermal stability [3]. The preparation of composite membranes of phosphosilicates with common electrolyte polymers such as Nafion has been proposed to maximize the fuel cell performances [4].

Solid acids are fundamental heterogeneous catalysts in several industrial processes [5]. Materials based on phosphate species supported on or mixed with silica, such as "solid phosphoric acid", show significant protonic (Brønsted) acidity, which has been exploited for a long time in oligomerization and alkylation reactions of hydrocarbons [6, 7]. In the transition from fossil feedstock to biomass-derived resources, that is, in the development of biorefineries, the large differences in the chemistry of the raw materials and in the reaction environment require suitable catalysts with enhanced water tolerance [5, 8]. Therefore, the low hydrolytic stability of Si–O–P linkages is a challenge to overcome, hence ensuring the durability of the catalysts.

Bioactive glass and ceramics exhibit biological activity through the formation of bonds with living tissue, especially with bone, by stimulating faster regeneration and supporting osteogenesis. SiO_2-P_2O_5 materials are suitable choices for tissue engineering, often combined with other oxides, above all CaO, because the bone structure is close to that of hydroxyapatite ($Ca_5(PO_4)_3OH$) [9–11]. Consequently, ternary and multinary oxide systems attract large interest as biomaterials.

Polymer-based composites, coatings, and fabrics used in everyday life and in industrial production generally require fireproof properties. The formation of inorganic phases in polymer matrices has been proven to be an effective approach to enhance their thermal stability and fire behavior and can also affect the mechanical properties and recyclability [12, 13]. The sol-gel process is particularly suitable for the modification of textile substrates with hybrid architectures, able to protect the surface of the fabrics by creating a barrier to heat and mass transfer that improves fire resistance [14]. Appropriately designed functional fillers containing both silicon and phosphorus provide a significant flame retardant action to the obtained composites, avoiding the use of halogen-based additives, which are responsible for the formation of toxic and corrosive combustion products [15, 16]. Therefore, in recent years research efforts have been devoted to the in situ formation of hybrid inorganic phases containing a network of Si–O–P linkages, particularly in epoxy nanocomposites, taking advantage of sol-gel chemistry [17, 18].

The preparation of phosphosilicate glasses was first carried out by traditional high-temperature melting [1]. In the 1990s, the sol-gel methodology acquired popularity also for the synthesis of phosphate-containing gels, including SiO_2-P_2O_5 [19–22], paving the way toward the development of homogeneous products with cross-condensation of Si and P-units and uniform distribution at the atomic scale. The sol-gel technique allows for operating in mild conditions, resulting in less energy-demanding processes with lower risks of volatilization of P species and usually larger surface area of the final materials. Nonhydrolytic sol-gel routes were proposed to form a well-cross-linked Si–O–P network, though only in strictly controlled conditions (i.e., inert and dry atmosphere) [23]. However, Si phosphates and phosphonates obtained by these nonaqueous procedures were still usually found to be very sensitive to water [24]. In hydrolytic sol-gel routes, a careful selection of the precursors, reaction parameters, and possible thermal treatments can provide a certain accuracy in defining

the structure and features of the resulting oxide. Furthermore, the sol-gel process can be easily coupled with suitable deposition and fabrication techniques to obtain coatings or desired meso-/macrostructures, e.g., dip coating, spin coating, evaporation-induced self-assembly, and rapid prototyping [10, 25]. However, the widely variable reactivity of the available P precursors, the not entirely negligible volatility of phosphate species, and, again, the instability of Si–O–P linkages in hydrolytic solution make the synthesis of these structures very challenging. As a matter of fact, inhomogeneities in the materials' composition and low or undefined degree of Si–O–P interconnectivity were often reported [22].

In this review, the chemical background and technological aspect of the above-described synthetic issue are explored, with an overview of the main application fields of Si–P oxide-based materials and of future research perspectives and expected developments.

2 Si–O–P linkages in solid materials

Silicon and phosphorus are the 2nd and 11th most abundant elements in the Earth's crust, making up about 27.2% and 0.1% of its mass, respectively [26]. Their main properties are collected in Table 1, which shows that despite having similar atomic weight and radius, the two elements have quite different electronegativity, also affecting the reactivity of their oxides. Silicon is naturally bonded to oxygen in a variety of silicate structures, based on 4-coordinated units [SiO_4], usually linked by shared corners (O atoms). Silicon dioxide (silica, SiO_2) and related materials have huge industrial importance: indeed, silica is a primary component of traditional ceramics, including concrete, brick, and glass, it is used in filtration, thermal insulation, surface passivation of silicon and other semiconductors, as an additive in composites, paints, cosmetics, food, and pharmaceuticals, as adsorbent and catalyst support, among others. In addition, siloxane networks with organic moieties constitute silicones, a widespread group of versatile polymers. SiO_2 is mostly found as quartz, a crystalline polymorph with rhombohedral symmetry, and less frequently as tridymite (orthorhombic) or cristobalite (tetragonal), two polymorphs that are metastable in ambient conditions.

Table 1 Main properties of silicon and phosphorus elements [156]

Property	$_{14}Si$	$_{15}P$
Atomic weight	28.085	30.974
Electron configuration	[Ne] $3s^2$ $3p^2$	[Ne] $3s^2$ $3p^3$
Electronegativity (Pauling)	1.90	2.19
Ionization energy (1st, kJ/mol)	786.6	1012
Electron affinity (kJ/mol)	134	72
Covalent radius (pm)	111	107

The most common oxide of phosphorus has empirical formula P_2O_5 and molecular formula P_4O_{10}, corresponding to the anhydride of phosphoric acid. The high affinity of phosphorus pentoxide to water, resulting in a vigorous reaction with the production of phosphoric acids, makes it useful as a desiccant and dehydrating agent [26]. Silicon phosphates, i.e., mixed oxides of Si and P, find applications in various sectors, including energy conversion and storage, optoelectronic devices, heterogeneous catalysis, adsorption, ion exchange and purification techniques, biomaterials and flame retardance (see Section 3). In the SiO_2-P_2O_5 system, a set of different structures can be obtained almost in the entire composition range, up to 80–90 mol% P_2O_5, generating a complex phase diagram [27]. The building units are generally [SiO_4] and [PO_4] tetrahedra, forming up to four and three oxygen bridges, respectively (as [PO_4] units have a non-bridging P = O double bond). However, some silicophosphates usually obtained at high temperatures can also contain hexacoordinate [SiO_6] structural units, giving different crystalline forms, such as silicon pyrophosphate, SiP_2O_7, and silicon orthophosphate, $Si_5O(PO_4)_6$. Both SiO_2 and P_2O_5 are network-forming oxides in glasses; however, $[PO_4]^{3-}$ does not show a tendency to reticulate producing gels, although it can form linear or cyclic polyphosphates (Fig. 1) [20].

In the early stages of the research on phosphosilicate glasses, these materials were prepared by high-temperature melting of parent oxides or precursors. Later, wet chemical methods, particularly sol-gel, took the stage as convenient and sustainable routes toward the preparation of gels and glasses; these processes are generally performed at room temperature and require a subsequent calcination treatment with the desired heating program. Thus, a much more accurate control of the procedure was attained, allowing for the synthesis of Si–P mixed oxides with excellent homogeneity. However, the choice of the right precursors and process parameters to maximize the Si–O–P connectivity, sought to enhance some key functional properties, is a challenge still open to advances (Fig. 1).

2.1 Hydrolytic (in)stability of Si–O–P linkages

The production of solids based on a uniform Si–O–P network by sol-gel is a complex task for two main related reasons: (a) the restricted ranges of reaction conditions that allow for the formation of these bonds, especially in hydrolytic processes; and (b) the limited stability of Si–O–P linkages in an aqueous environment and even in contact with atmospheric humidity. Hence, once these bridges have been obtained by cross condensation of Si and P units, the reverse reaction (hydrolysis) occurs quite easily:

$$\equiv \mathrm{Si} - \mathrm{O} - \mathrm{P} \equiv + \mathrm{H_2O} \rightleftharpoons \equiv \mathrm{Si} - \mathrm{OH} + \equiv \mathrm{P} - \mathrm{OH} \quad (1)$$

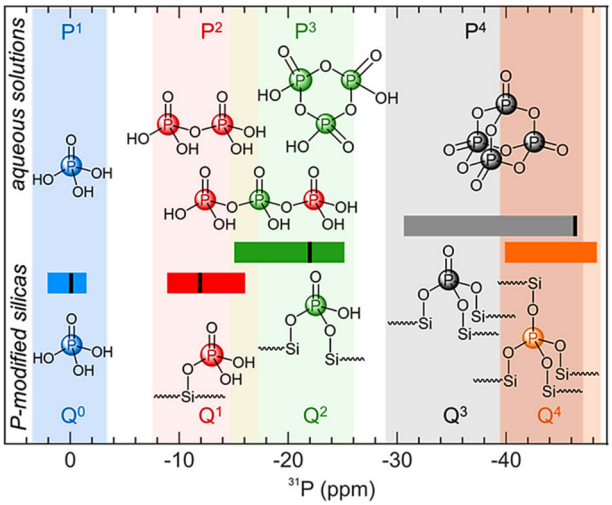

Fig. 1 Structures of possible P units in polyphosphates in solution (P_n sites) and P–Si solid oxides (Q_n sites) and the corresponding typical chemical shift values (for P_n) and ranges (for Q_n) in ^{31}P NMR spectroscopy. Reprinted with permission from [101]. Copyright 2021 American Chemical Society

This weakness is attributed to the strong affinity of phosphorus to water. The average bond energy of Si–O is 452 kJ/mol, while that of P–O is 335 kJ/mol, both having the same average bond length (163 pm) [26]. Contrary to the high symmetry and low reactivity of [SiO_4] tetrahedral units, [PO_4] tetrahedra are slightly asymmetric (because of the shorter phosphoryl bond, P = O), which implies that a non-zero dipole moment is present in cross-linked phosphate units. Phosphorus has also a larger tendency to expand its coordination, favoring the nucleophilic attack by water and the subsequent substitution through the breaking of a P–O bridging bond. The protonation of the resulting Si–O^- group completes the formation of a Si–OH (silanol) and a P–OH group. Silanols can then condense to Si–O-Si bridges, promoting phase separation. This difference in reactivity is in agreement with that observed between the two oxides: P_2O_5 reacts vigorously with water, giving phosphoric acids, while SiO_2 is considered insoluble and highly stable in water. However, it should be noted that silica is not completely unaffected by water, and, particularly in the case of mesoporous silica-based materials, the large surface areas and low mass content of the porous matrices make them quite susceptible to undergoing chemical, textural, and structural modifications by interaction with water, which may also result in some leaching in solution (as silicic acid). In this regard, it was reported that preparing mesostructured silica mixed with alumina or zirconia (up to 10 mol%) [28] or P_2O_5 (up to 5 mol%) [29] via evaporation-induced self-assembly reduces the release of silicate species in water at 37 °C, increasing also the biocompatibility of the materials.

The formation of Si–O–P links can be revealed by ^{31}P solid-state NMR [21, 30, 31], infrared and Raman spectroscopies [32, 33]. The spectroscopic features related to these bonds can be found close or partly overlapped by other characteristic bands or signals of Si–O–Si or P–O–P linkages, so their assignment should be done carefully. X-ray photoelectron spectroscopy (XPS) can also give information on the connectivity at the surface of the material through the analysis of the 2p signals of Si and P [34]. In general, the growth of extended Si–O–P networks by typical hydrolytic sol-gel procedures depends on the molecular precursors, composition of the system, hydrolysis ratio (i.e., the water concentration), solution pH, drying temperature, and possible annealing/calcination treatment of the gel. The most common molecular precursors of P in the sol-gel synthesis of Si–P oxides are shown in Fig. 2. Their different reactivity is reflected in their different ability to form Si–O–P linkages as well as in their variable stability. Phosphoric acid, despite being quickly hydrolyzed in an aqueous solution, shows a limited propensity to condense with silanol groups, which is related to the weak nucleophilicity of P–OH groups and the small positive partial charge on the P atom [20]. Thus, in the ^{31}P solid-state NMR spectra of gels synthesized using H_3PO_4 as a precursor, the Q_0' signal, corresponding to the unreacted acid adsorbed or weakly bonded to the silica matrix, usually prevails [30, 35]. On the other hand, triethyl phosphate (TEP) has extremely slow kinetics of nucleophilic substitutions at room temperature and neutral pH, hindering the polycondensation reactions.

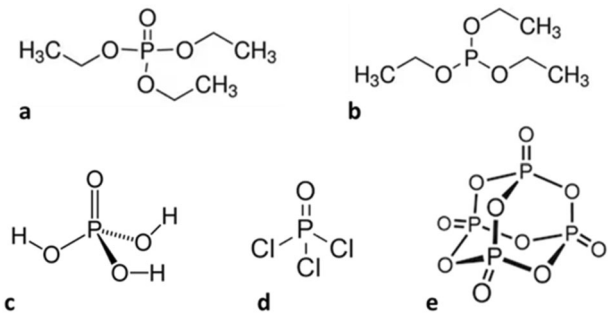

Fig. 2 Molecular structure of the most used phosphorus precursors: (**a**) triethyl phosphate (TEP), (**b**) triethyl phosphite (TEPI), (**c**) orthophosphoric acid, (**d**) phosphoryl chloride, (**e**) phosphorus pentoxide (P_2O_5)

With the aim of overcoming the difficulties in the successful preparation of silicophosphates with homogeneous distributions of Si and P in aqueous environment, non-hydrolytic routes were also proposed [24]. In this context, Styskalik et al. [23] adopted a nonaqueous route through ester elimination at low temperature starting from silicon acetate, $Si(OAc)_4$, and tris(trimethylsilyl) phosphate, $OP(OSiMe_3)_3$, and obtained amorphous xerogels with high condensation degree (up to 87.5%) and large surface areas, containing hexacoordinate silicon units [SiO_6] in their structure. The so-obtained xerogels appear still highly sensitive to hydrolysis of the Si–O–P bonds when they come in

contact with water [36]. The main drawbacks of nonaqueous processes are the strictly controlled conditions required, i.e., inert and dry atmosphere, and the generally more complex structure of the employed precursors.

The effect of washing in water was tested on phosphate-modified silicate gels prepared by addition of H_3PO_4 after acid prehydrolysis of tetraethoxysilane (TEOS). In the sample dried at 100 °C, H_3PO_4 appeared to be loosely bonded to the matrix and was removed by repeated treatments in water at room temperature, whereas after calcination at 600 °C the stability in water was improved: this finding was likely due to the formation of a polyphosphate surface layer with some Si–O–P linkages [37]. Phosphosilicate structures containing [SiO_6] octahedral units connected to [PO_4] tetrahedra in the presence of a network modifier like Na_2O show increased stability, as recently proven by the reduced chemical dissolution of P-Si-Ca-Na glasses in a buffer solution at 37 °C [38]. The formation of such structures possibly represents an approach toward the enhancement of the hydrolytic resistance of Si–O–P networks.

2.2 Thermally-induced formation and thermal stability of Si–O–P linkages

As already mentioned, thermal treatments are crucial in determining the structure and cross-condensation degree in phosphosilicate materials, since heating can induce further polycondensation and phase transitions. Silica-based gels are generally amorphous after drying; then, heating can promote the growth of different crystalline phases. The increase in the degree of condensation after the thermal treatment is evidenced by the evolution of the ^{29}Si and ^{31}P NMR spectra of xerogels treated at increasing temperatures (Fig. 3). Moreover, it was shown that in xerogels that do not contain Si–O–P linkages, their formation can be triggered at a relatively low temperature, such as 200 °C [21]. The temperature required for increasing the formation of Si–O–P bridges and the extent of cross-linking changed with the P content and its precursor (see also Section 3). For example, in gels prepared using TEOS and $POCl_3$ with 10 mol% and 30 mol% P_2O_5, after treatment at 300 °C only the latter sample showed evidence of the formation of Si–O–P linkages by solid-state ^{31}P NMR spectroscopy, while the former required higher temperatures [30]. Amorphous gels prepared from TEOS and H_3PO_4 initially exhibited a high P content in the outer layer, suggesting a precipitation of phosphate on the surface, while thermal treatment induced the crystallization of P-rich phases in the bulk and Si-enrichment of the surface, with the formation of Si–O–P linkages [34]. In gels obtained from H_3PO_4 with P/Si molar ratio of 1/10, heating up to 900 °C was needed to observe a marked change in the ^{31}P NMR spectrum, attributed to condensed phosphate units involved in Si–O–P bonding, whereas using TEP provided only a distribution of Q_0' and Q_1' P units [35]. The positive effect of heating on the formation of Si–O–P linkages is likely associated with the activated condensation of vicinal hydroxyl groups, as supported by the observed reduction of –OH concentration estimated in colloidal silica gels containing P-modified aerosil, according to the following scheme [39]:

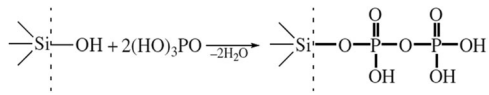

On the other hand, it must be noted that some phosphorus compounds have a non-trivial volatility, which can limit the thermal stability of the solids containing these phases. The resistance to loss by volatilization is strongly related to the P precursor. Various studies agree that P losses increase when unreactive precursors, such as TEP, are used. For instance, among the gels with high P_2O_5 content (70–90 mol%) heated at 800 °C, the samples prepared from H_3PO_4 and $P(OCH_3)_3$ (trimethyl phosphite) retained most of their P, while those derived from TEP lost a large fraction of P [21]. This observation was confirmed for gels with 10 mol% P_2O_5 prepared with three different precursors. After annealing at 700 and 1000 °C, the P_2O_5/SiO_2 ratios in the glasses derived from H_3PO_4 were found to be 1.89 and 1.94 times higher, respectively, than in the TEP-derived counterparts. It was suggested that TEP interacts with the silica gel mainly by physisorption and that it is partially volatilized and degraded during the thermal treatment [40]. The lability of incorporated P might be emphasized in thin films, as reported for phosphosilicate films with a thickness of a few hundred nm prepared by dip coating from sols containing 10 mol% P_2O_5 with H_3PO_4, TEP, and TEPI ($P(OC_2H_5)_3$) as sources [41]. XPS analysis highlighted a dramatic evaporation of the P alkoxide between 200 and 500 °C, leading to almost total loss of surface P, while H_3PO_4 produced more stable P species. A lower homogeneity of the composition resulting from the synthesis normally facilitates phase separation phenomena and thus encourages the loss of volatile species at high temperatures.

3 Synthesis and applications of materials based on Si-P oxides

About 30 years ago, hydrolytic sol-gel replaced the conventional high-temperature ceramic route as the preferred synthesis method for Si–P mixed oxides. Several studies dealt with this process, exploring how the variables affected

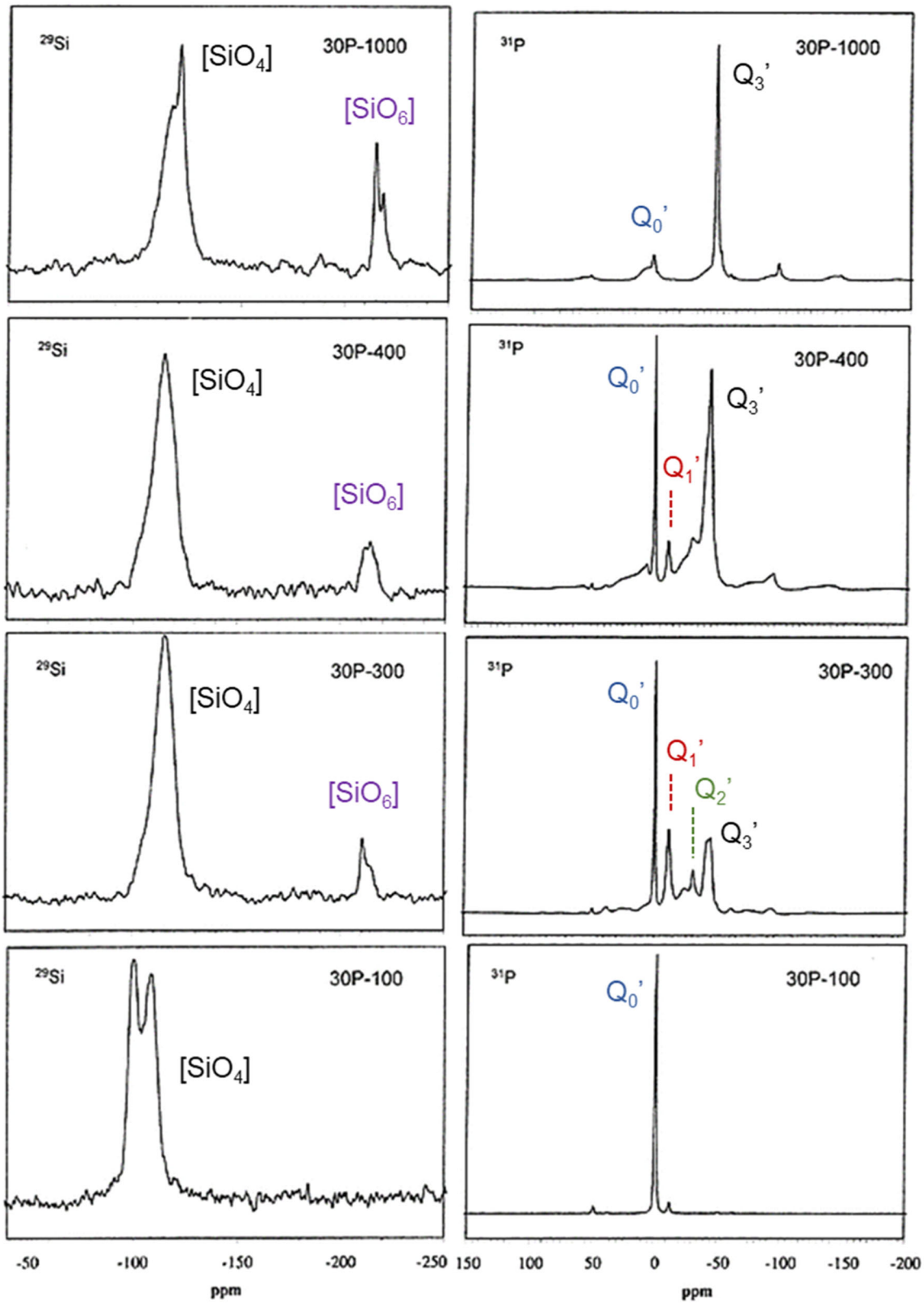

Fig. 3 ^{29}Si (left) and ^{31}P (right) MAS NMR spectra of Si–P gels containing 30% P_2O_5 (30P) treated at different temperatures (100, 300, 400 and 1000 °C), with the indication of the Si- and P-units corresponding to the different bands. For ^{31}P spectra the resonances lying outside −5 to −50 ppm are spinning sidebands. Adapted and reproduced with permission from [30], copyright 2001 Royal Society of Chemistry

its progress and outcome. The P_2O_5 precursor was soon identified as a crucial factor in determining both the reaction rate, the extent of polymerization, and the properties of the final product. While TEOS was almost invariably chosen as Si precursor, different molecular precursors of P have been considered, mostly those illustrated in Fig. 2. The huge differences in the hydrolysis and condensation rates of these compounds have been already mentioned. Specifically, phosphate esters, $PO(OR)_3$, react too slowly with water under ambient conditions to be easily used as the precursors of P_2O_5, whereas orthophosphoric acid reacts too fast with respect to TEOS, therefore it can lead to precipitation rather than gelation. To grow a homogeneously cross-linked structure with a fine dispersion of each phase into the other, the hydrolysis and condensation rates of the precursors need to be well-matched. Alternative precursors with intermediate reactivity are the mixed compounds obtained by dissolving phosphoryl chloride, $POCl_3$, or P_2O_5 in alcohols, forming different $PO(Cl)_{3-x}(OR)_x$ or $PO(OH)_{3-x}(OR)_x$ species. In these species, the partial positive charge of the P atom lowers, thus reducing its reactivity toward water. Another interesting alternative is phytic acid, a natural non-toxic compound derived from plants, which was successfully introduced in a silica matrix. The gels deriving from phytic acid showed the appearance of some Si–O–P linkages after heat treatment and maintained a good capacity to chelate metal ions [42, 43].

A few attempts to use silica sources different than TEOS in the synthesis of Si–P binary oxides were reported. Sodium silicate (Na_2SiO_3) was used with $ZrOCl_2$ and H_3PO_4 to prepare zirconium silicophosphate [44], while a commercial suspension of colloidal silica nanoparticles was reacted with H_3PO_4 to form a sol for the deposition of antireflective coatings [45]. Natural minerals were also proposed, for example metakaolin or a sand sample, both collected in Tunisia; before the reaction with H_3PO_4, the former was activated in HCl [46], while the latter was converted into sodium silicate and then into silica gel [47].

Several comparative studies available in the literature on the structure of phosphosilicate gels and films depending on the P precursors evidence the complexity of these relationships, generally agreeing on the main outcomes, as summarized in Section 2.2. Most works focused on TEP, H_3PO_4, and sometimes TMP and TEPI as P sources [35, 40]. Wang et al. [48] prepared sols and gels by directly reacting P_2O_5 with TEOS, finding an improved cross-condensation and retention of phosphorus in the phosphosilicate structure and the appearance of six-coordinated $[SiO_6]$ units in the amorphous gel obtained by aging at temperature as low as 70 °C. They argued that P–O–Si linkages are formed by the gradual addition of Si-OEt groups onto bridging oxygens of P_4O_{10} clusters in anhydrous conditions, before water addition. On the other hand, the presence of six-coordinated silicon and $[SiO_4]$ tetrahedra linking $[PO_4]$ tetrahedra in the glassy matrix of a silicophosphate gel-derived glass obtained in hydrolytic conditions was first observed by Clayden et al. [30] in the $30P_2O_5{\cdot}70SiO_2$ glass heated in air at 300 °C. From this glass, the crystallization of phases containing hexacoordinated silicon, i.e., $Si_5O(PO_4)_6$ and $Si(HPO_4)_2{\cdot}H_2O$, occurred at higher temperatures. In any case, whatever strategy is adopted in the synthesis procedure to match the reactivity of Si and P precursors, this does not overcome the key point of the synthesis, i.e., the intrinsic instability of the Si–O–P linkages in an aqueous environment. Therefore, the gels obtained at about room temperature are mainly formed by condensation of siloxane clusters, originated by the growing of silicon oligomeric species, that include P species, metaphosphoric or orthophosphoric acid, according to the extent of the following equilibrium [49]:

$$HPO_3 + H_2O \rightleftharpoons H_3PO_4 \quad (2)$$

An effective strategy to overcome this trade-off is to add a third component, such as niobium: this latter accounts for the stabilization of Si–O–P linkages as a consequence of the formation of Si–O–Nb bridges that allowed for a stable anchoring of phosphorus through the formation of Nb–O–P bonds within the gel [50, 51].

As a matter of fact, many applications of mixed oxides containing Si and P, including proton conductivity, optical and biological activity, and acid catalysis, benefit from the presence of other metals giving rise to ternary or quaternary oxide systems. Typical cases are represented by titanium or zirconium phosphates tested in PEMs for fuel cells (see Section 4.1), niobium included in Si–P catalysts for enhanced acidity (see Section 4.2), and calcium phosphate silicate bioceramics for tissue engineering. The presence of network modifiers may play a crucial role in determining the structural features of the oxides. For example, phosphosilicate glasses fabricated by melt-quenching and containing alkali cations (Na_2O molar fraction within 0.1 and 0.4) exhibit superstructural units, in which Si is mainly in the form of $[SiO_6]$ octahedra, connected with six $[PO_4]$ tetrahedra by shared corners, with Na^+ ions compensating the charge (Fig. 4). In these structures with medium-range order, predicted on the basis of solid-state NMR data, Si–O–P linkages are therefore stabilized owing to the alkali cation [52, 53]. Theoretical results supported this type of structure through molecular dynamics modeling of modified silicophosphate glass, indicating that the content of $[SiO_6]$ and the distribution of $[PO_4]$ is related to the Na_2O and CaO content. Also, the larger stability of this structure was proven by the suppressed chemical dissolution in a buffer solution at 37 °C [38]. Moreover, it was shown that adjusting the content of octahedral Si units can increase the glass transition temperature, hardness, and refractive index

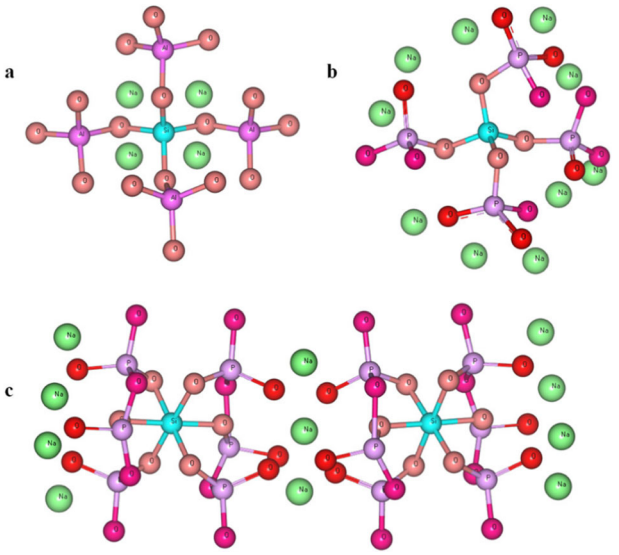

Fig. 4 Representation of the connectivity in: (**a**) [SiO_4] units in nepheline, an aluminosilicate mineral; (**b**) [SiO_4] units in Na_2O-P_2O_5-SiO_2 glasses; (**c**) superstructural units containing [SiO_6] species, each connected with six [PO_4] units (stoichiometry: $Na_2SiP_6O_{18}$). Reprinted with permission from ref. [53]. Copyright 2018 American Chemical Society

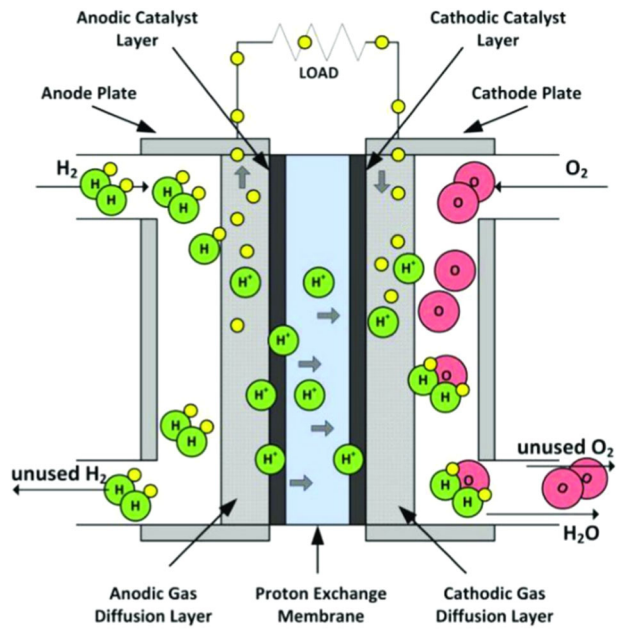

Fig. 5 Schematic representation of a Proton Exchange Membrane (PEM) fuel cell and its functioning principle. Reproduced with permission from [155]. Copyright 2014, Elsevier

of Si–P glasses, widening their applicability [54]. On the other hand, hexacoordinated Si found in a silicophosphoric acid glass with high P/Si ratio, produced by melt-quenching and alkali-proton substitution, was presumed to be responsible for the low proton conductivity of the material because of the trapping of H^+ carriers around the [SiO_6] units [55].

In the following, the main application sectors of Si–P oxide-based materials and nanostructures are reviewed. Bioactive glasses and ceramics are of great interest in biomedicine and particularly in bone tissue engineering, owing to their ability to bind to the tissues, stimulating faster regeneration and supporting osteogenesis [10]. Again, the choice of precursors and synthesis conditions are fundamental in determining the texture, porosity, and biocompatibility of these materials. Since these oxide systems in most cases consist of three or more elements (typically Si–P–Ca, resembling supported hydroxyapatite [11, 56]), they are not extensively treated in the present work.

3.1 Phosphosilicate glasses and films in electrochemical and optical devices

Glasses and films with phosphosilicate structure have important applications in fuel cells and in some optical devices. Most fuel cell technologies using hydrogen or methanol rely on a PEM to separate fuel and oxidant (see Fig. 5). PEM fuel cells are very promising options for low-carbon transport, especially for heavy-duty and long-range transportation. Efficient PEMs require specific characteristics, including high and stable proton conductivity, adequate water uptake and swelling rate, and high chemical and thermal stability. Direct methanol fuel cells, having the advantage of a liquid fuel, which is easier to store and transport than hydrogen, additionally need low methanol permeability [57]. Despite the fast progress in the field of PEM fuel cells, technological challenges remain, such as retaining high proton conductivity at high temperatures and low relative humidity (RH), in order to increase the power density, and reduce mechanical and chemical degradation [2]. High-temperature operation (over 120 °C) is potentially desirable for PEM fuel cells because of the advantages offered at this operating temperature; on the other hand, humidity is essential, as water promotes the diffusion of protons through the membrane.

An overview of proton conduction in sol-gel glasses was recently published [3]. The most accredited proton transport mechanism in oxides, called the "hopping" or Grotthuss mechanism, involves a transfer of H^+ from one site to the adjacent through hydrogen bonds, though a detailed interpretation of the process is still debated. Glasses show proton transport also in dry conditions, as the protons can move between non-bridging oxygens in the bulk of the material. However, the activation energies for proton hopping through molecular water are lower than for hopping between these oxygens, therefore proton conductivity is enhanced when the pores contain water. The transfer of protons in a glass membrane is believed to stem mainly from their hopping of protons through the hydrogen-bonded water and hydroxyl groups in the network structure (see

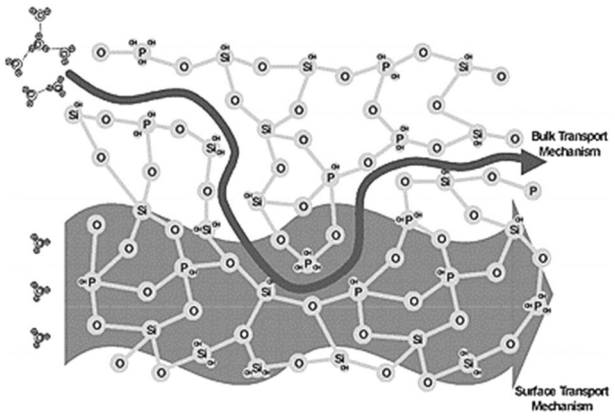

Fig. 6 Representation of proton conductivity mechanism in a Si–P glass membrane, showing the prevalence of surface transport over bulk transport. Reprinted with permission from [68]. Copyright 2005, Royal Society of Chemistry

Fig. 6). The proton in a P–OH group is strongly H-bonded with water and more mobile compared with the proton of a Si–OH group, which explains the increase in conductivity when P_2O_5 is mixed with silica. Proton conduction in phosphosilicate glasses was investigated in several pioneering works by Nogami's research group [58–62]. In these materials, the conductivity generally increases with both temperature and water concentration, reaching typical values up to about 10^{-2} S/cm at room temperature and 60–70 % RH. The activation energy estimated for the proton conduction through hopping involving water molecules in the glasses is about 10 kJ/mol at high RH [60]. The distribution of different phosphorus species in a mixed oxide is clearly related to the proton conductivity. A heterogeneous distribution of P units in the silicate matrix is often observed in phosphosilicate gels. A detailed 2-dimensional NMR magnetization exchange spectroscopy study by Clayden et al. [63] revealed a chemical heterogeneity at the nanoscale in $10P_2O_5$-$90SiO_2$ gels and highlighted the effects of ^{31}P–^{31}P and ^{1}H–^{31}P dipolar coupling. Monomeric P was found near to P–O–P crosslinks, while doubly cross-linked P units were found isolated from other P species. ^{31}P spin exchange indicated a weak dipolar coupling between Q_0 and Q_1P and no exchange peaks to Q_2 were observed. The results were attributed to three spin interactions involving ^{1}H spins and a hydrogen bond interaction between Q_0 and Q_1 units, in agreement with the association of these units. Proton dynamics at different sites in phosphosilicates was further investigated by means of muon spin relaxation as a function of temperature, using the positively charged muon as a probe since it behaves as a light isotope of the proton [64]. Since proton transport occurs preferentially on the surface of the pore channels, the conductivity is also affected by the porosity, namely the pore size, volume, and surface area. For P_2O_5-SiO_2 gel-derived glasses, low conductivity values were recorded for glasses having pores larger than about 15 nm, because these are hardly filled with water molecules independently of the humidity, while high proton conductivity occurred in glasses with smaller pores diameter, being optimal for pore size between 2 and 4 nm [62, 65].

The sol-gel method is particularly suitable for the production of proton-conducting materials because the nanostructure can be accurately directed and because the micropores in the gels can be easily filled with liquid that promotes fast proton transport, in contrast to melting techniques that produce less porous solids. A reference phosphosilicate glass studied by Nogami and co-workers [58, 60] had nominal molar composition $5P_2O_5$-$95SiO_2$ and was synthesized by hydrolysis of TEOS and $PO(OCH_3)_3$ with a small amount of HCl, the addition of a variable volume of formamide to control the porosity, and a final heat-treatment of the gel at 600 °C for 2 h. Matsuda et al. [66] prepared xerogels with larger P content from TEOS and H_3PO_4 (P/Si molar ratio up to 1.5), treated at 150 °C. They reported proton conductivities in the same order of magnitude (10^{-2} S/cm), with P/Si equimolar ratio as optimal composition. A sufficient conductivity was also recorded at low RH (20%). The same authors also used TEP and a single Si–P precursor, namely 2-(diethoxyphosphoryl)ethyltriethoxysilane (DPTS). Interestingly, moving from H_3PO_4 to these P source, the maximum conductivity was observed at increasing calcination temperatures (300 °C for TEP, 450 °C for DPTS). Increments in the conductivity values were associated with a larger number of isolated orthophosphoric acid sites in the samples [67]. This observation is in agreement with a larger contribution of less condensed phosphoric sites with more available P–OH groups. Glasses with P_2O_5 content between 10 and 50 mol% were obtained from TEOS and TEP at 60 °C in saturated air, a procedure leading to accelerated gelation, followed by sintering up to 700 °C. The pore size distribution was dependent on the composition, as well as the conductivity and methanol permeability, with a maximum selectivity (the ratio of the conductivity to permeability) reaching a maximum in the $30P_2O_5$-$70SiO_2$ glass membrane [68]. The advent of ordered mesoporous silicas inspired the synthesis of ordered bimodal hexagonal mesoporous phosphosilicate monoliths, using TEOS, trimethyl phosphate (TMP), and Pluronic P123 as template [69]. Modified sol-gel methodologies were proposed to produce phosphosilicate PEMs. Monolithic and transparent membranes were synthesized from TEOS and H_3PO_4, and subjected to hydrothermal treatment at 150 °C for 30 h. Proton conductivities of 10^{-1} S/cm were achieved, which is comparable to those of commercially available polymeric membranes, such as Nafion [70].

Despite the relatively high proton conductivity and selectivity of phosphosilicate glasses employed as PEMs, their performances and stability need to be enhanced to

meet the requirements for commercialization. This can be fulfilled by coupling them with either inorganic materials, such as transition metal oxides and heteropolyacids, or ion conductive polymers. Transition metal phosphates (e.g., zirconium and titanium phosphates) with layered structure and heteropolyacids, like phosphotungstic acid, $H_3PW_{12}O_{40}$ (HPW or PTA), with Keggin structure, show very good proton conductivity, adequate for their incorporation in inorganic glass membranes. For example, the introduction of ZrO_2 or TiO_2 gave porous ternary Si-Zr-P and Si-Ti-P with various molar compositions (e.g., $30P_2O_5$-$10ZrO_2$-$60SiO_2$, $40P_2O_5$-$20ZrO_2$-$40SiO_2$, $9P_2O_5$-$6TiO_2$-$85SiO_2$), having large surface area and improved chemical and mechanical stability [71–74]. Phosphate-based heteropolyacids, particularly HPW, can greatly enhance proton conductivity at both low and high temperature if appropriately immobilized on a support, such as mesoporous silica [75]. Aricò et al. [76] studied the effect of the surface properties of different ceramic oxide fillers (SiO_2, HPW-impregnated SiO_2, ZrO_2, Al_2O_3) on recast Nafion composites applied in direct methanol fuel cells. They found that the surface acid-base properties of the fillers play a crucial role in determining the conductivity characteristics at high temperature (145 °C) and the fuel cell performance (maximum power density), which was ascribed to the improved water retention by acidic OH groups on the particle surfaces.

Rather than competing to replace polymeric electrolyte membranes with inorganic ones, the most effective approach toward high-performing fuel cells seems to be their integration into hybrid organic-inorganic composite membranes [4, 77, 78]. Perfluorosulfonic ionomers, chiefly Nafion, have been the state-of-the-art PEM for fuel cells operating at low temperatures for a long time. The insertion of phosphosilicate-based particles into the polymer matrix was performed by different methods, generally using TEOS and H_3PO_4 as precursors: for example, via the infiltration of Nafion membrane with the oxide sol after pretreatment in H_2O_2 and H_2SO_4 or the mixing of the sol with Nafion solution followed by recasting, drying and washing [71], possibly aided by a hydrothermal treatment of the mixed Si-P/Nafion gel [79]. Mistry et al. [80] developed Nafion-phosphosilicate hybrid membranes combining solvent-directed infiltration with sol-gel chemistry using organo-functional precursors like phytic acid. The phase-separated morphology of Nafion acted as a structure-directing template, driving the inorganic component into the ionic clusters of the polymer, with the formation of Si–O–Si and Si–O–P linkages observed by photoacoustic FTIR spectroscopy. To obtain flexible, chemically, and thermally resistant composite membranes it is fundamental to ensure good compatibility between the components and a uniform dispersion of the filler. Functionalized inorganic-organic oligomers can also be prepared by condensation of TEOS and other precursors with polydimethylsiloxane (PDMS), carefully adjusting the reaction parameters [81], while methacrylate-phosphosilicate hybrids can be synthesized by polymerization from suitably modified P and Si alkoxides [82].

Sulfonated poly(ether ether ketone) (SPEEK) and polybenzimidazole (PBI) are efficient alternative polymeric electrolytes for PEMs, increasingly studied in the last years also as composites embedding inorganic phases. Li's research group fabricated phosphosilicate/SPEEK composite membranes by a simple mechanical mixing of sols prepared from TEOS and H_3PO_4, aided by ball milling. The products exhibited satisfactory mechanical properties (flexibility and tensile strength) even with inorganic content as high as 40–50 wt.%. The incorporation of phosphosilicate sol remarkably enhanced the conductivity of SPEEK. The membranes with an optimized composition reached a maximum proton conductivity of 0.138 S/cm, at 70 °C and 95% RH (see Fig. 7) and peak power density about 450 mW/cm^2 at 60 °C [83]; they were also tested in the range 180–250 °C at different humidities [84]. Zhang et al. [85] developed a composite membrane based on polybenzimidazole doped with phosphoric acid and HPW-impregnated mesoporous silica. They recorded excellent durability operating at high temperature (200 °C), which was explained by a structural breakdown of the HPW-SiO_2 framework, forming in situ phosphosilicate phases within the PBI matrix. These nanoclusters, immobilizing part of H_3PO_4, provided high proton conductivity (up to $7.2 \cdot 10^{-2}$ S/cm) and inhibited acid leaching out of the membrane, simultaneously reducing the detrimental effect of excess acid on the agglomeration of Pt catalyst in the cathode layer and thus increasing the operational stability.

Ternary oxides were also loaded onto polymer electrolytes. Castro et al. [86] produced hybrid organic-inorganic membranes with functionalized SiO_2, TiO_2-P_2O_5 or SiO_2-TiO_2-P_2O_5 gel particles through an elaborated sol-gel procedure. First, meso/macroporous oxide particles were obtained from TEOS, TMP and Ti(IV) isopropoxide, using Pluronic P123 and polystyrene foams as templates. Then, the oxide particles were modified with a functionalized silicon precursor, i.e., (3-methacryloxypropyl)trimethoxysilane (MPS) and an organic monomer (hydroxyethyl methacrylate, HEMA), with the aim of increasing the cross-linking degree of the network. The hybrid sols constituted by these oxide-MPS-HEMA particles with the addition of HPW were finally deposited by automatic spraying onto glass paper substrates. The proton conductivity of the composite membrane increased with temperature, reaching $2 \cdot 10^{-2}$ S/cm at 120 °C, owing to water retention in the network, suggesting the development of this strategy for medium-high temperature fuel cells [86]. Hybrid

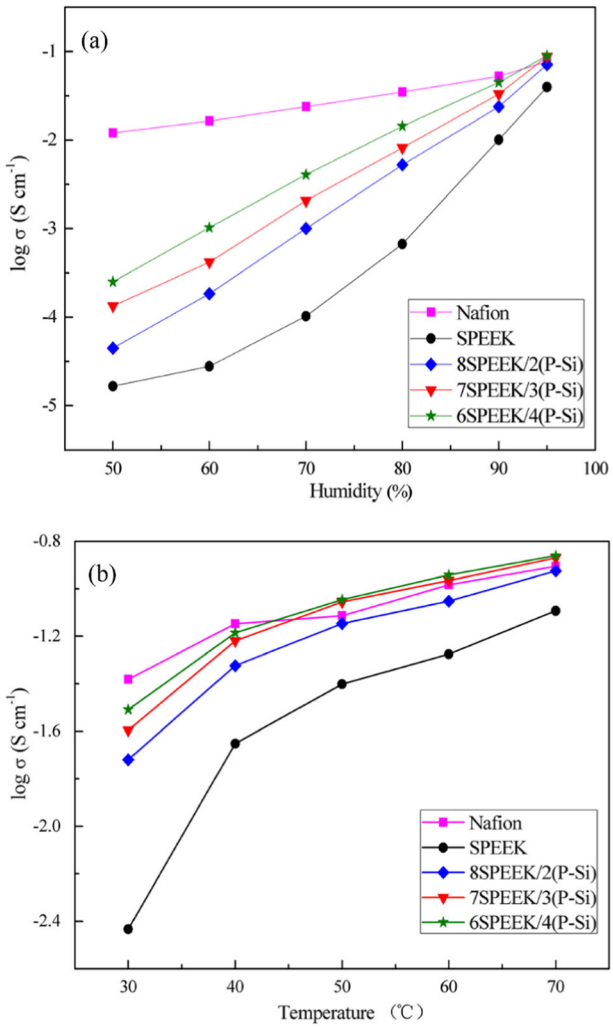

Fig. 7 Proton conductivity (σ) of SPEEK membrane, Nafion 212 membrane and phosphosilicate/SPEEK composite membranes with different molar ratios between the polymer and inorganic phases: (**a**) as a function of relative humidity (RH) at 50 °C; (**b**) as a function of temperature under 95% RH condition. Reprinted with permission from [83]. Copyright 2015, Elsevier

membranes were also prepared by mixing poly(methyl methacrylate) (PMMA) and Si-P oxide, with or without zirconia, through hydrolysis and condensation of TEOS, TMP and Zr(IV) propoxide [87]. For the best performing system (60PMMA-30SiO_2-10P_2O_5), proton conductivity of $3.85 \cdot 10^{-1}$ S/cm at 90 °C and 50% RH and a stable current density were recorded.

Recently, sulfonated styrene-ethylene-butylene-styrene (sSEBS) membranes were modified by infiltration with a Zr-Si phosphate sol prepared from TEOS, TMP and Zr(IV) propoxide (40SiO_2-40P_2O_5-20ZrO_2) [88]. The composite membrane showed improved thermal stability and stiffness, lowered water and methanol uptake, and increased conductivity and power density compared to bare sSEBS, suggesting potential applications in direct methanol fuel cells with reduced methanol crossover. In another recent research effort, Siekierski et al. [89] studied a phosphosilicate glass synthesized with two polymeric additives, namely, poly(ethylene oxide) (PEO) and poly(vinyl alcohol) (PVA), and incorporating a titanium oxide filler, either as commercial nanopowder or grown in situ by hydrolysis and condensation of Ti(IV) ethoxide. The pore distribution and surface area of the glass were clearly altered by the additives, and the analysis of the dispersion of dielectric losses through electrochemical impedance spectroscopy (EIS) in dry and wet conditions led the authors to argue that the composites exhibit mixed-type proton mobility with contributions from both the bulk of the material and the surface of the pores.

The high affinity of phosphates to water has been exploited in some research works to construct resistive humidity sensors. Phosphosilicate thin films prepared from TEOS and $POCl_3$ by dip coating were tested by EIS, revealing a strong influence of P content and heating temperature on the sensitivity to RH in the range 57–90 % owing to a protonic sensing mechanism [25]. Organic-inorganic nanocomposites were prepared by mixing a TEOS-H_3PO_4 sol with different polyionenes, i.e., polymers with charges residing along their backbones. The fractal characteristics of the nanocomposites were examined by means of TEM and small angle X-ray scattering, observing that ultrasound treatment of the sols caused a decrease in the dimensions at different structural levels. The values of alternating current conductivity were quite sensitive to RH in the range 23.5–96.5 % [90]. P_2O_5-SiO_2 binary glass derived from TEOS and TMP was also proposed as an electrochemical sensor of hydrogen gas: the sample was placed between two porous Pt electrodes, measuring the electromotive force as a function of hydrogen partial pressure, and it was found to be an efficient Nernstian gas sensor [59]. A novel attractive application for phosphosilicate nanomaterials, based on their protonic conduction and electronic insulation, was recently proposed by MIT researchers, who fabricated a protonic programmable resistor compatible with complementary metal-oxide semiconductor, using a 10 nm phosphosilicate film deposited by plasma-enhanced chemical vapor deposition (CVD) as solid electrolyte layer [91]. The device showed low energy consumption, symmetric and durable conductance modulation, opening perspectives for advances in technology of analog crossbar processors for deep learning.

Phosphosilicate glasses have been extensively employed as host matrices for immobilization because of their excellent optical transparency, physical rigidity, high photochemical and thermal stability, and negligible swelling in organic solvents. Their optical properties, such as the transmittance in the UV-visible-NIR range and the refractive index, are affected by the composition and sintering

temperature of the gels [92]. Optical waveguides allow for the confined transmission and propagation of light through large distances with negligible intensity losses. Planar waveguides are needed in various devices and as interconnects for photonic integrated circuits. Nanocomposites of phosphosilicate with a hyperbranched polyamidoamine polymer containing Er^{3+} complexes were prepared by hydrolysis and condensation of TEOS and TEP, followed by mixing with the polymer and erbium nitrate. Monoliths and films were obtained respectively by casting in a mold and spin coating. The high refractive index of the hybrid material (about 1.83) and the room temperature NIR photoluminescence make it interesting for the development of planar optical waveguides [93]. Semiconductor quantum dots may benefit from the dispersion in a host matrix as well, since it improves their photochemical and thermal stability leading to high-performance LEDs. For example, $CsPbBr_3$ and $CsPbBr_2I$ perovskite quantum dots were embedded into phosphosilicate glasses produced by melt-quenching and thermal treatment, resulting in increased stability and lifetime of the light emitters [94, 95]. Furthermore, phosphosilicate optical fibers were proposed for use in radiation sensing and dosimetry, based on the phenomenon of radiation induced attenuation. A P-doped single mode optical fiber produced by a CVD method was recently assessed and calibrated for gamma-rays, X-rays, and proton irradiation, and given the positive results it was selected for implementation in some parts of the Large Hadron Collider at CERN (European Organization for Nuclear Research) [96].

3.2 Si-P oxide-based catalysts

Solid acids have a key role in heterogeneous catalysis. The interest in the exploitation of phosphoric acid and its derivatives in industrial catalytic processes by the immobilization on a solid support dates back to the 1930s, when "solid phosphoric acid" (SPA) was introduced for the production of gasoline through the oligomerization of light olefins. SPA is traditionally produced by impregnation of H_3PO_4 onto kieselguhr (diatomaceous earth), followed by calcination at high temperature. The product may contain a variety of active P species, including orthophosphoric, pyrophosphoric ($H_4P_2O_7$), and polyphosphoric acids, on a mixture of silica and Si phosphates acting as the support [6, 97]. Two related issues are commonly encountered operating with this kind of catalytic materials: a low tolerance to water and humidity, causing severe hydrolysis and leaching of P species in wet environment, and a limited mechanical strength of the particles, whose breakdown can be associated with reduced catalyst lifetime. In the last decades, some studies have attempted to contrast these problems by modifying the preparation procedure of SPA. The control of the composition of the Si-P phases produced was found to be crucial, and a balance between silicon ortho- and pyrophosphate ($Si_5O(PO_4)_6$ and SiP_2O_7) allowed for the improvement of the activity and stability of the catalysts, tested in the alkylation of benzene and oligomerization of alkenes [7, 97, 98].

The significant Brønsted acidity of Si–P mixed oxides, mostly due to the acidic character of P–OH groups (much stronger than that of Si–OH groups) has stimulated the development of materials containing Si–O–P phases as main active species or catalyst supports, often combined with metals or metal oxides/phosphates. The composition and related microstructure of silicophosphates influence their acid properties. Gels with P_2O_5 content from 5 to 30 mol%, were prepared from TEOS and $POCl_3$ in an almost pure aqueous solution and treated at 400 °C [49]. The sample with 5 mol% P_2O_5 showed the largest surface area, the smallest pore size, and the highest concentration of free phosphoric acid; increasing the P fraction decreased the surface area, a transition from micro- to mesopores occurred and more condensed P units were observed. The characterization of the surface acidity by temperature programmed desorption (TPD) of ammonia evidenced a trend also in the distribution of acid sites (see Fig. 8). The TPD profiles indicated the presence of Brønsted acid sites of differing strength, mainly related to phosphoric acids, while SiO_2 gave only a limited amount of acid sites, corresponding to a low temperature peak. The surface concentration and strength of acid sites were found to increase with P content, although the density of acid sites per unit mass reached a maximum at 10 mol% P_2O_5.

In the conventional refinery processes, strong protonic acid solids have been developed to activate crude oil

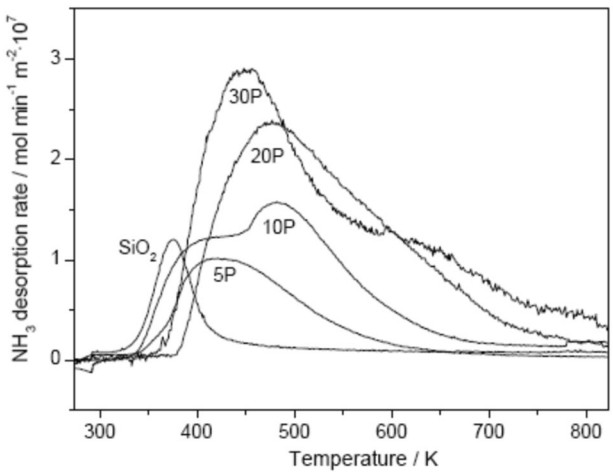

Fig. 8 NH_3 temperature programmed desorption profiles of SiO_2 and Si–P oxide gels with different P_2O_5 mol% (5, 10, 20 and 30 mol%), heated for 1 h at 400 °C. Reprinted (adapted) with permission from ref. [49]. Copyright 2005 American Chemical Society

hydrocarbons due to their weak basic character. Nowadays, heterogeneous catalysis is a key technology in the necessary transition from a chemistry based on fossil raw materials to a more sustainable chemistry based on biomass feedstock. According to the more polar nature and larger oxygen content of renewable raw materials (e.g., lignocellulose), catalysts with weaker protonic acidity or mixed Brønsted-Lewis acidity may be needed [5]. Moreover, the different reaction environment and conditions (water solution or at least polar reagents and solvents) require catalysts with enhanced water tolerance and, therefore, the development of new solid acids with suitable properties.

Phosphosilicate catalysts have been frequently prepared by multistep procedures, i.e., grafting or impregnation of phosphoric acid on a pre-formed silica or mixed silicate structure, similar to SPA production. A kind of SPA was prepared based on aluminum-loaded SBA-15 mesoporous silica and tested in cellulose fast pyrolysis. The post-synthesis deposition of Al on the support resulted in an increased yield of bio-oil and levoglucosenone, an added-value product. The formation of Al phosphates changed the selectivity of the reaction and reduced the amount of easily leachable H_3PO_4, which could delay the deactivation of the catalyst [99]. A SiO_2-supported Ni(II) obtained by electrostatic adsorption was modified with excess H_3PO_4 and subsequent calcination and tested in high-temperature alkane dehydrogenation reactions. The introduction of phosphate provided single-site tetrahedral Ni(II) phosphosilicate as an efficient catalyst in propane dehydrogenation, owing to the activation of the C–H bond by Ni–OSi groups and to the role of Ni–OP bonds in preventing the reduction of Ni(II) to Ni(0) under the dehydrogenation conditions, thus helping to achieve high stability and selectivity [100].

Phosphorus-modified zeolites possess remarkable acid catalytic properties that can be useful in biorefinery processes. For instance, P-containing siliceous zeolites, or P-zeosils, catalyze the selective dehydration of biomass derivatives to platform chemicals such as p-xylene and 1,3-butadiene. These reactions generate water, which is a critical factor in the catalytic activity, whose effects are not fully understood yet. A silica-based pillared P-zeosil with a low P-loading (Si/P = 27) was studied by solid-state ^{31}P NMR, via Dynamic Nuclear Polarization of a variety of P sites, including mononuclear and dinuclear sites, associated with P–O–Si and P–O–P linkages [101]. The more condensed sites evolve rapidly when exposed to humidity, even at room temperature, forming partially hydrolyzed P species, affecting the overall acidity. Hydrolysis generates a mixture of partly reacted monomeric and oligomeric sites and therefore a new distribution of Brønsted acid sites. Similarly, zeolite Beta and hierarchical MFI zeolite were modified with phosphorus, the former, after dealumination, by impregnating H_3PO_4, the latter by a direct synthesis method using tetrabutylphosphonium hydroxide as a structure-directing agent. The calcined P-containing zeolites were successfully tested in the Diels-Alder cycloaddition of 2,5-dimethylfuran and ethylene and the subsequent dehydration of the cycloadduct intermediate, which represent an attractive reaction pathway toward selective p-xylene production from biomass feedstocks [102].

The development of specific morphologies can widen the catalytic potential of Si–P oxides, as in the case of fibrous phosphosilicate (FPS) particles, synthesized in a microemulsion system with tripolyphosphate (TPP) and TEOS as precursors, and urea and cetylpyridinium bromide (CPB) as additives. After a hydrothermal treatment at 120 °C, mesoporous FPS were obtained, consisting of dendritic fibers expanded radially outward, providing a high surface area and high accessibility of the reactant by a host-guest approach. The nanomaterials showed pronounced ionic internal character, good thermal stability, and long-term colloidal stability. FPS was used to support different active species aiming at the utilization of carbon dioxide, namely: Pd nanoparticles for the cycloaddition of CO_2 to several epoxides [103], an aluminum layer for its cycloaddition to terminal alkenes [104], producing in both cases cyclic carbonates, and a ruthenium complex for the photocatalytic conversion of CO_2 to formate under visible light irradiation [105]. An attractive application in the field of energy vectors was recently proposed for Si–P oxides, namely the production of hydrogen from the hydrolysis of sodium borohydride ($NaBH_4$). Ganesan et al. [106] prepared phosphorylated silica starting from TEOS and H_3PO_4 and found a significant and stable H_2 generation efficiency from $NaBH_4$ solution. The kinetic and thermodynamic study of the reaction suggested that a Langmuir–Hinshelwood associative mechanism occurs in the hydrolysis of borohydride at the catalyst surface, promoted by the exposed phosphoric acid groups.

Non-hydrolytic sol-gel processes carried out in well-controlled conditions offer interesting alternative routes for the production of functionalized silicophosphates. Styskalik et al. [107] synthesized a variety of Si–P porous xerogels by the reaction of acetoxysilanes with trimethylsilyl esters of phosphoric and phosphonic acids, resulting in cross-linked networks with homogeneously dispersed Si and phosphoryl units connected by Si–O–P linkages. The functional properties of the products were sensitive to the organic substituents and the Si/P ratio of the precursors. Further, the reaction of the residual organic groups with silicon, phosphorus or aluminum compounds enriched the surface of these materials with additional Brønsted (P–OH) and Lewis (tetracoordinated Al) acid sites. The catalytic performances of the modified silicophosphate xerogels were tested in the dimerization of methylstyrene, achieving excellent activities and moderate to high selectivities, which suggested their potential suitability for this type of reactions [36].

According to the results described so far, the design of ternary oxides, in which Si, P, and a transition metal are uniformly mixed appears as a promising way to obtain systems with tailored catalytic properties. Synthesis procedures involving a separated step of phosphoric acid wet impregnation have been widely adopted [108, 109] and few works have reported the direct synthesis of ternary oxides by hydrolytic sol-gel for catalytic purposes. An example of this approach is the synthesis of a silicon-titanium phosphate performed using TEOS, Ti(IV) butoxide, and trimethyl phosphite, in an ethanol solution of acetic acid, concentrated HCl, and Pluronic F127 as a structure directing agent [110]. The calcined gel was active in the acid-catalyzed Friedel-Crafts benzylation reaction of aromatics and in the adsorption of toxic metal ions. A different route was used for the preparation of a zirconium silicophosphate (ZSP) deposited on pectin gel starting from zirconium oxychloride, sodium silicate and H_3PO_4 [44]. By stirring the aqueous solution of precursors at pH 0–1 and 50 °C, ZPS precipitates were formed, then pectin gel led to the final nanocomposites, where the polysaccharide acted as binder for ZSP nanoparticles. The material exhibited high ion exchange capacity, allowing for the separation of binary solutions of some metal ions, the ability to remove methylene blue dye from solution by adsorption combined with solar light photocatalysis, and some antimicrobial activity.

In the open challenge to extend the durability of the catalysts in water environment, overcoming the low hydrolytic stability of Si–O–P linkages, and to modulate the nature and strength of acid sites, the introduction of niobium into the phosphosilicate network is very promising. Niobium oxophosphate, $NbOPO_4$, is, indeed, a reference solid acid, as niobium forms both Lewis ([NbO_4] tetrahedra) and Brønsted (Nb–OH groups on [NbO_6] octahedra) sites, as depicted in Fig. 9. Aronne's research group [50] established a synthesis route of Nb-P-Si ternary oxides from niobium chloride, $NbCl_5$, phosphoryl chloride and TEOS. The structural characterization of gels with Nb_2O_5 and P_2O_5 content between 2.5 and 10 mol% treated at 500 °C highlighted an extended cross-condensation with formation of Si–O–Nb–O–P bridges that allowed for a stable anchoring of phosphorus within the matrix (see Fig. 9). The materials showed remarkable catalytic performances in different biomass valorization reactions, namely the hydrolysis of inulin (a plant-derived polysaccharide), the dehydration of fructose to 5-hydroxymethylfurfural and the esterification of fatty acids with polyalcohols [111–113]. Interestingly, the samples with lower content of active phase (i.e., 2.5 mol% P_2O_5 and 2.5 or 5.0 mol% Nb_2O_5) had the highest activity, likely due to the large specific surface area and the availability of less polymerized P units providing strong Brønsted acidity. The analysis of the density, strength, and distribution of acid sites of the Nb-P-Si oxides revealed that a high concentration of both Lewis and Brønsted acid sites are active in the vapor phase, while in water the latter sites prevail, suggesting a significant effective acidity that was mainly preserved after washing in water [112, 113]. The leaching of P species during the water treatment was neatly decreased by doubling the Nb/P ratio, supporting the role of the metal in anchoring phosphorus [113]. In addition, to increase the compliance of the synthesis process of Nb-P-Si materials with the principles of green chemistry, a new sol-gel route was developed. This one-pot procedure occurs in water at room temperature, employs safe and inexpensive compounds (namely, H_3PO_4 and ammonium niobium oxalate) in place of the chloride precursors, and does not require any catalyst, additive, or organic solvent [51]. The annealing at 500 °C in air completes the cross-linking of the amorphous porous structure. The medium-strong Brønsted and Lewis acidity, revealed by the surface characterization, leads to an interesting catalytic activity in the gas-phase conversion of ethanol to ethylene, with a high selectivity at 250–300 °C, a simultaneous dehydrogenation pathway to acetaldehyde at higher temperature, and an unusually low yield of diethylether, a common by-product of the reaction [114]. Overall, the design of ternary oxides containing a Si, P, and a transition metal is a viable way to obtain catalytic materials with enhanced performances and stability.

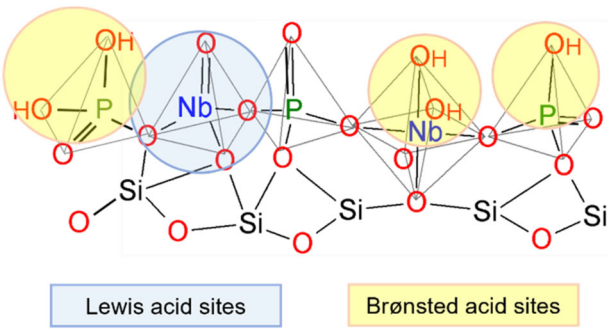

Fig. 9 Schematic representation of acid sites on the surface of a Nb-P-Si ternary oxide

3.3 Si-P structures in inorganic polymers

Inorganic polymers are a class of polymers with backbones that do not include carbon. For this reason, these polymers combine the advantages of organic molecules with those of inorganic solids. Some examples of inorganic polymers are polyphosphazenes and polysiloxanes [115–117]. The derivatives of such polymers with controlled molecular weight and structure have been exploited as flame retardants, tissue scaffolds and drug carriers [118]. Polysiloxanes are largely used for their high thermo-oxidative stability and low-temperature flexibility [119]. In this framework, several research groups

have investigated the possibility of bringing a P–Si synergistic effect of flame retardation in inorganic polymers and related materials. By reaction of pentaerythritol dichlorophosphate (i.e., 3,9-dichloro- 2,4,8,10-tetraoxa-3,9 diphosphaspiro[5,5] undecane 3,9-dioxide) with oligosiloxanes, it was possible to synthesize a macromolecular flame retardant. It was composed of a polymer chain built up from siloxane blocks and spirocyclic segments linked by phosphate groups. Also, orthophosphoric or phenylphosphonic acid can be used for the preparation of low melting glasses with O-P-O-Si chain building segments. The preparation procedure involves the reaction with chlorotrimethylsilane (CTMS) or methyltrichlorosilane at elevated temperatures up to 200 °C [120]. As previously highlighted, the development of effective synthesis methods to link Si and P in linear polymers represents a very challenging task. Feasible strategies can be adapted from polymerization techniques used in the preparation of organic macromolecules with incorporated inorganic blocks [121]. Linear O–P–O–Si chains were obtained via a polycondensation process normally exploited in the preparation of poly(-alkylene H-phosphonate)s derived from diesters of the H-phosphonic acid. In 1959, Kohlschütter and Simoleit [122] described the reaction between the diesters of methylphosphonic acid and CTMS. Later, the same reaction was applied by Rabinowitz [123] to various phosphonates, though a temperature as high as 70 °C and long reaction times were necessary to achieve good yields with CTMS. In particular, the conversion of dimethyl methylphosphonate into the corresponding ditrimethylsilyl methyl-phosphonate took almost 6 h, while phosphonates with bulky substituents required several weeks to achieve satisfactory yields. The formation of a phosphonium-type Arbuzov intermediate was considered in the proposed mechanism for the reaction (see Fig. 10).

Several studies carried out on the reactivity of dialkyl esters of H-phosphonic acid have proved that the α-carbon atom of the alkoxy group is also a potential site of nucleophilic attack, which makes the alkyl phosphonates able to take part in the dealkylation reaction [124, 125]. Based on

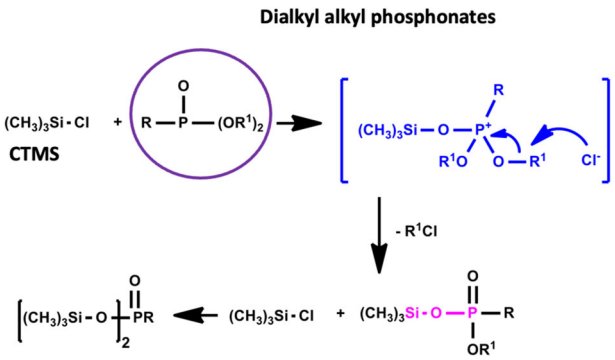

Fig. 10 Proposed mechanism for the synthesis reaction of linear O-P-O-Si chains, also involving the formation of a phosphonium-type Arbuzov intermediate [126]

that and on the above mechanism, Mitova et al. [126] obtained a phosphorus- and silicon-containing inorganic polymer, with a linear chain structure (i.e., [-O-P(O)(H)-O-$Si(CH_3)_2$-]) and building units of reactive P-H groups, through the reaction between dimethyl ester of H-phosphonic acid (DMP) and dichlorodimethylsilane (DMDCS) at a molar ratio of 1.3:1. The research group prepared the inorganic polymer without using any catalyst or solvent and the process was performed in two stages at temperatures up to 65 °C under inert atmosphere. Mitova et al. [126] confirmed the chemical structure of the inorganic polymer by solid-state NMR spectroscopy. They also elucidated the reactions taking place in the two stages: (i) a dealkylation step between the α-carbon atoms of DMP (dialkyl H-phosphonate) and DMDCS (i.e., the silane promoting the nucleophilic attack), and (ii) a polycondensation leading to an increase of the molecular mass of the final product.

3.4 Si-P structures in hybrid organic-inorganic polymers and nanocomposites

The in-situ generation of inorganic phases in polymers has been widely used as a valuable approach for obtaining organic-inorganic (hybrid) composites with enhanced thermal stability and fire behavior. Silica nanoparticles and other similar structures (i.e., polyhedral oligomeric silsesquioxanes) can be formed in the polymer network starting from suitable precursors, such as tetraethyl orthosilicate (TEOS) [127–129]. It is well known that, during the combustion of polymer-based materials, silica nanoparticles can promote the formation of a very stable char acting as a thermal shield [130, 131]. Modern society continues to demand more multifunctional products in the field of laminates, casting, and electronic components, for which low flammability and good mechanical properties are highly desirable. Epoxy resin is one of the most exploited polymer matrices in the manufacturing of such products, due to its high adhesion and chemical resistance [132, 133]. The epoxy resin market size was estimated at USD 22.9 billion in 2021 with a compound annual growth rate (CAGR) of 7.3% from 2022 to 2030 [134, 135]. On the other hand, epoxy resins usually exhibit poor fire resistance and their combustion releases toxic smoke and flammable gases, which limits their widespread application [136, 137]. There are several strategies to improve the flame retardance of epoxy resins involving either the modification of the polymer matrix or the addition of a proper flame-retardant additive, and sol-gel chemistry represents a feasible and effective approach in both cases. In addition to silicon-based structures, functional fillers containing phosphorus provide excellent flame retardant features to epoxy resins and enable the use of halogen-based additives to be avoided, which generate toxic and corrosive combustion

products [138]. The possibility to incorporate both silicon and phosphorus in the epoxy network obtaining a synergistic effect in the enhancement of both thermal behavior and flame retardancy has been deeply investigated [13, 139].

In particular, many efforts were devoted to obtaining in situ hybrid inorganic phases characterized by a stable network of Si–O–P linkages in the polymer matrix of nanocomposites, although the intrinsic instability of these bonds toward water is the key aspect that needs to be faced [49]. The chemical modification of the polymer matrix takes place by reaction with an appropriate Si-containing precursor, such as a silane, and then a P-based additive is used to promote the formation of Si–O–P linkages in the char obtained from the combustion of the nanocomposite. When Si–O–P substructures are formed in the carbonaceous char, the heat provided during the combustion is responsible for the formation of bonds between -P-OH and -Si-OH reactive groups by condensation [13, 139].

Bifulco et al. [129, 140] prepared aliphatic silica-epoxy nanocomposites through a sol-gel strategy, using TEOS and (3-aminopropyl)triethoxysilane (APTES) as precursors for the in situ synthesis of silica nanoparticles. They obtained self-extinguishing systems by the incorporation of P-based flame retardants (i.e., 6H-dibenz[c,e][1,2]oxaphosphorin,6-[(1-oxido-2,6,7-trioxa-1-phosphabicyclo[2.2.2]oct-4-yl) methoxy]-, 6-oxide and 3-(6-oxidodibenzo[c,e][1,2]oxaphosphinin-6-yl) propenamide) and melamine into the polymer matrix. The chemical analysis of the residual char revealed that its superior insulating properties arise from the presence of inorganic substructures including Si–O–P linkages (Fig. 11) [130, 141]. Within a waste-to-wealth approach, Venezia et al. [142] modified an epoxy resin with APTES, and used humic acid (HA), as bio-waste flame retardant, in combination with ammonium polyphosphate (APP) to achieve self-extinguishing behavior. The synergism of HA and APP promoted the formation of an intumescent char, containing N−P−O−Si chains, which acted as a protective barrier for heat and oxygen.

Many attempts were performed to obtain hybrid polymers with networked stable Si–O–P linkages by sol-gel, even if the clear evidence of such bonds in the final structure of nanocomposite was proved only recently by ^{31}P solid-state NMR measurements [18]. The sol-gel synthesis of hybrid polymers containing Si- and P-based structures often requires the use of organic solvents, as these solvents allow for creating suitable microenvironments in the hydrophobic polymer, where silicon- and P-based moieties can interact forming substructures. An epoxy hybrid was obtained by a sol-gel procedure involving different precursors of N, P, and Si in tetrahydrofuran, which showed higher values of the thermal degradation activation energy than the unmodified epoxy counterpart [143]. Chang and

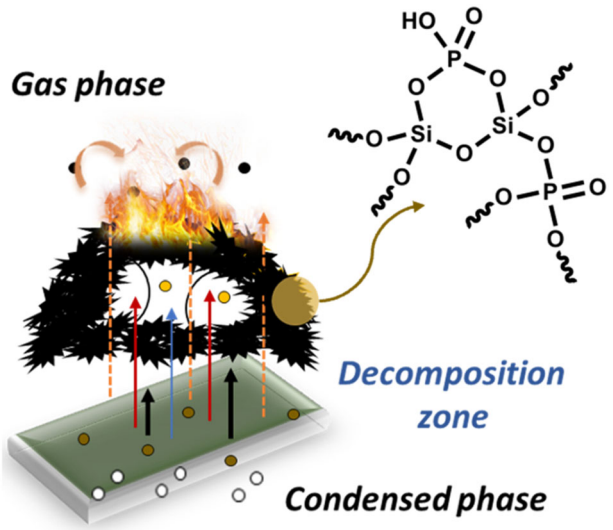

Fig. 11 Si-O-P substructures formed during the combustion of epoxy-silica nanocomposites containing phosphorus-based flame retardant [130]

Ma [144] prepared hybrid epoxy nanocomposites by treating a bisphenol A diglycidyl ether (DGEBA) resin with TEOS, a coupling agent, i.e., (3-isocyanatopropyl)triethoxysilane, and (2-diethylphosphatoethyl)triethoxysilane (DPTS). They performed the sol-gel chemical modification of DGEBA by using tetrahydrofuran in a hydrolytic process and cured the resin with 4,4'-diaminodiphenylsulfone. The hybrid nanocomposites exhibited very good fire behavior and the epoxy network was characterized by solid-state ^{29}Si NMR, showing the presence of Q_4, Q_3, T_3 units.

Recently, Parida et al. [145] synthesized hybrid silica nanoparticles starting from TEOS and a phosphonate-based nonsilane (i.e., N,N´-Bis[4,6-bis(diethylphosphono)-1,3,5-triazin-yl]-1,2-diaminoethane) as P precursor in aqueous environment. The presence of Si–O–P substructures was attributed to physisorption of -PO(OH)$_2$ groups with -Si–OH moieties (Fig. 12).

Recently, Bifulco et al. [18] prepared Si–P hybrid nanocomposites via a hydrolytic sol-gel route. The synthesis process involved a pre-reaction of DGEBA resin with APTES and subsequent condensation of hydroxyls by TEOS at 80 °C (Fig. 13).

To prevent a fast crosslinking of the epoxy chains, the phosphorus precursor, i.e., phosphoric acid, was added at room temperature through a solution containing ethanol. After that, the mixture was cured with isophorone diamine hardener. The strategy exploited by the research group promoted the formation of Si–O–P linkages in the epoxy matrix, avoiding the use of toxic solvents and aromatic phosphorus-based precursors. The functionalization of DGEBA resin by APTES led to the generation of silanized epoxy chains, which rearranged in nanodomains, after the addition of ethanol and water, that

acted as nanoreactors for the hydrolysis and condensation of the precursors (i.e., phosphoric acid and TEOS). This mechanism promoted the establishment of Si–O–P links in the hydrophobic environment of the polymer matrix and resulted in a co-continuous organic-inorganic (i.e., epoxy-silica) network made of uniformly dispersed lamellar silica nanocrystals (obtained without surfactant templates), with a multi-sheet morphology, containing P-moieties. The Si–P hybrid nanocomposites did not exhibit dripping phenomena during UL-94 vertical flame spread tests; in addition, a notable reduction (up to 27.7%) in the peak of heat release rate (PHRR) was observed, together with the formation of a huge amount of char after combustion [18].

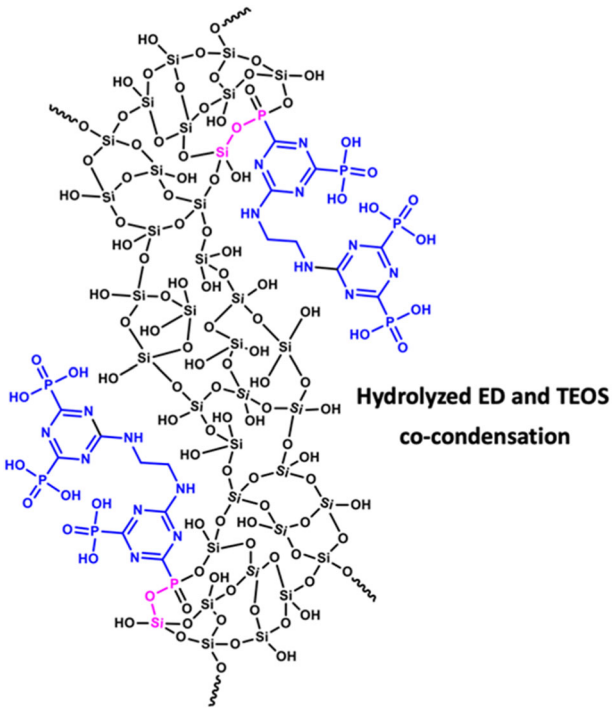

Fig. 12 Si–O–P substructures in hybrid networks formed by co-condensation of TEOS with ED (N,N´-Bis[4,6-bis(diethylphosphono)-1,3,5- triazin-yl]-1,2-diaminoethane) [145]

3.5 Si-P systems in surface coatings and textile treatments

The combination of silicon and phosphorus has been quite extensively employed for designing new flame retardant coatings, obtained by means of sol-gel chemistry or UV-induced polymerization, for the protection of fabrics or, less frequently, bulk polymers [14].

Textile materials are usually flammable polymers (if not inherently fireproof), showing a very irregular and complex-shaped surface, which makes it difficult to cover with an effective flame-retardant coating. In this context, in situ sol-gel reactions have been used to promote the formation of ceramic or hybrid organic-inorganic coatings (based on the composition of the applied sol solution), able to slow down flame propagation or protect the underlying substrate from a direct irradiative heat flux [12, 146, 147]. The literature reports several nice examples of using sol-gel derived

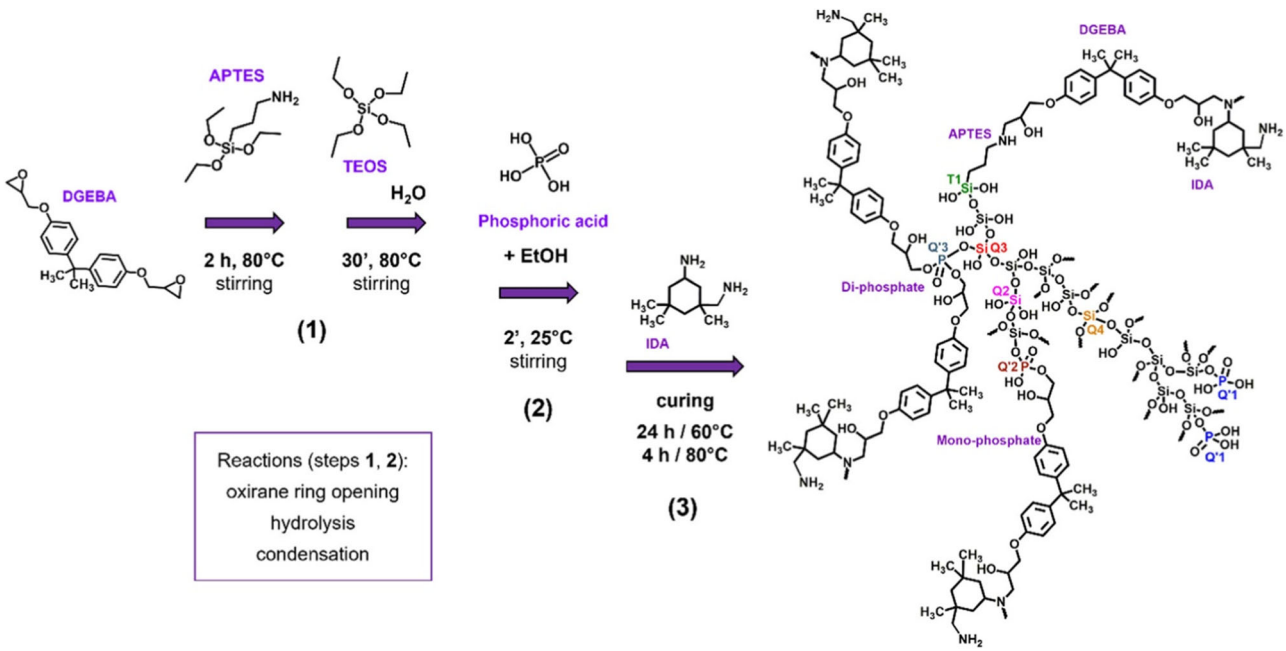

Fig. 13 Hydrolytic sol-gel route for the preparation of Si–P-epoxy hybrid nanocomposites and representation of their chemical structure. Reprinted with permission from ref. [18]. Copyright 2023 American Chemical Society

ceramic-based (often oxidic) coatings suitable for conferring flame-retardant features to different textile substrates. Two main approaches are considered, namely (i) the embedding of phosphorus-based flame retardants into the sol-gel derived coating and (ii) the "doping" of sol-gel derived coatings with phosphorus, usually covalently linked to the ceramic network (this way, phosphorus is first linked to the alkoxysilane precursor through a chemical bond, and then participates in the buildup of the sol-gel coating). The former strategy, despite high effectiveness in providing flame retardant features to the treated textile substrate, shows some drawbacks, specifically referring to the sometimes-limited durability of the fireproof characteristics, due to the washing out of the P-based flame retardant when the fabrics are subjected to laundry cycles.

As an example, Brancatelli and co-workers [148] impregnated cotton fabrics with hybrid sols derived from the combination of APTES and diethylphosphite (1:1 molar ratio; after drying 19 wt.% final add-on). As confirmed by the ASTM D1230 standard, the treated fabrics were self-extinguishing: the flame instantly extinguished upon the removal of the ignition source, leaving behind a very small, charred area. However, after 5 washing cycles performed in accordance with the EN ISO 6330:2000 standard, diethylphosphite was hydrolyzed and removed, hence indicating some durability issues with the proposed coatings.

Alongi et al. [149] applied sol-gel-derived silica coatings to cotton fabrics, starting from tetramethoxysilane as silica precursor, and embedding two commercially available phosphorus-based flame retardants, namely Exolit® OP1230 (aluminum phosphinate) or Exolit® OP1312 (a mixture of 63.5 wt.% aluminum phosphinate, 32 wt.% melamine polyphosphate, and 4.5 wt.% zinc and boron oxide); the phosphorus flame retardant loading was varied between 5 and 30 wt.% and the final dry add-ons after the sol-gel process were in between 19 and 24 wt.%. The concurrent presence of the ceramic phase created by the alkoxysilane and the phosphorus flame retardants accounted not only for an overall enhancement of the thermal and thermo-oxidative resistance but also for the achievement of self-extinction in both horizontal and vertical flame spread tests. In particular, the fabrics treated with the sol-gel-derived silica coatings and embedding 15 wt.% of the flame retardants burnt out after 2 s from the application of the flame. Further, notwithstanding the lack of chemical bonds between the silica coating and the phosphorus flame retardants, the treated fabrics were able to withstand a laundry cycle at 60 °C for 1 h in bi-distilled water, without significant changes in their fire behavior.

Chen and co-workers [150] prepared a novel phosphorus-rich hybrid organic-inorganic silica coating, for enhancing the fire behavior of silk fabrics, combining phytic acid and TEOS as phosphorus and silica precursors,

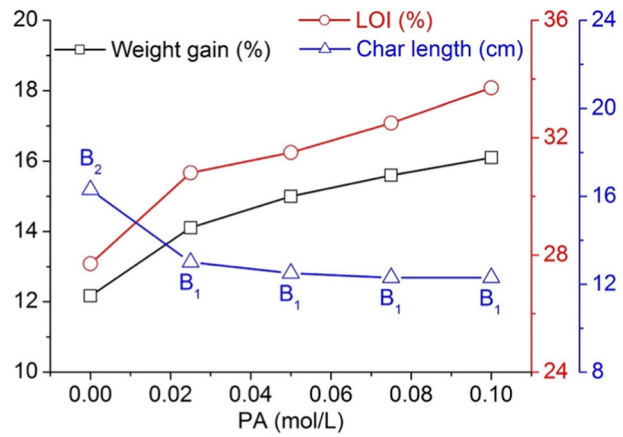

Fig. 14 Weight gain and flame-retardant performance (in terms of Limiting Oxygen Index – LOI, and vertical flame spread tests – Char length) of sol-gel-treated silk fabrics containing different amounts of phytic acid (PA). B_1 classification: char length ≤ 15 cm, after flame time ≤5 s, afterglow time ≤5 s; B_2 classification: char length ≤ 20 cm, after flame time ≤15 s, afterglow time ≤15 s. Reprinted with permission from ref. [150]. Copyright 2018, Elsevier

respectively. Further, aiming at improving the washing fastness of the sol-gel-treated fabrics, three silane coupling agents, namely (3-chloropropyl)trimethoxysilane, (3-aminopropyl)dimethoxymethylsilane, and MPS, were added in the hybrid sols. Flammability tests (Fig. 14) clearly demonstrated that the concurrent presence of the ceramic phase and the P-rich molecule accounted for self-extinction in vertical flame spread tests and increased Limiting Oxygen Index (LOI) values with increasing phytic acid content. Further, the introduction of silane coupling agents in the silica network enhanced the immobilization of the coating on silk substrate, hence improving the washing fastness of the treated fabrics.

Concerning the doping of sol-gel derived coatings with phosphorus covalently linked to the ceramic network, in one of the first pioneering works, Cireli et al. [151] compared the flame retardant properties provided to cotton fabrics by sol-gel coatings based on pure silica or P-doped silica phases. For the latter, either phosphoric acid or ethyl-dichloro phosphate was selected and added to TEOS; the final dry add-ons achieved after the sol-gel process on cotton were 24.5 and 20.6 wt.%, respectively. The fabrics treated with P-doped (using phosphoric acid) sol-gel-derived coatings achieved self-extinction in vertical flame spread tests; conversely, the fabrics coated with P-doped coatings based on ethyl-dichloro phosphate did not self-extinguish but exhibited longer flame spread times (i.e., about 20 s) with respect to both the fabrics coated with pure silica coatings (about 16 s) and the untreated counterparts (around 5 s). It is worth noting that the flame-retardant features were partially maintained even after 10 laundry cycles carried out according to the TS EN ISO 105-C06-A1S

standard, hence indicating some durability of the deposited sol-gel formulations.

Pursuing this research, Yaman [152] designed and applied hybrid P-doped sol-gel-derived coatings on polyacrylonitrile woven fabrics. H_3PO_4 was chosen as P-doping agent and bonded to the silica network obtained from TEOS precursor; three different TEOS to H_3PO_4 molar ratios were selected, namely 0.01: 0.17/0.34/0.5. As assessed by vertical flame spread tests, the treated fabrics exhibited self-extinction, with the only exception being the lowest P-doped formulation (i.e., that exhibiting TEOS:H_3PO_4 molar ratio of 0.01:0.17). Further, self-extinction was maintained even after 10 washings cycles for the fabrics treated with the highest TEOS:H_3PO_4 molar ratio.

Castellano et al. [153] succeeded in synthesizing a P-doped sol-gel precursor, namely *N*-(phosphonomethyl imino bis{2-hydroxy-3-[3-(triethoxysilane propoxy]propyl acetate]} (PGPTES) starting from (3-glycidyloxypropyl) triethoxysilane (GPTES) and a nitrogen-containing carboxyphosphonate (namely, *N*-(phosphonomethyl) iminodiacetic acid, PMIDA, Fig. 15). The obtained precursor was applied to cotton fabrics, by means of a sol-gel process (final dry add-on on the fabrics: 25.2 wt.%).

As highlighted by horizontal and vertical flame spread tests (Fig. 16), the P-doped sol-gel-derived coating achieved

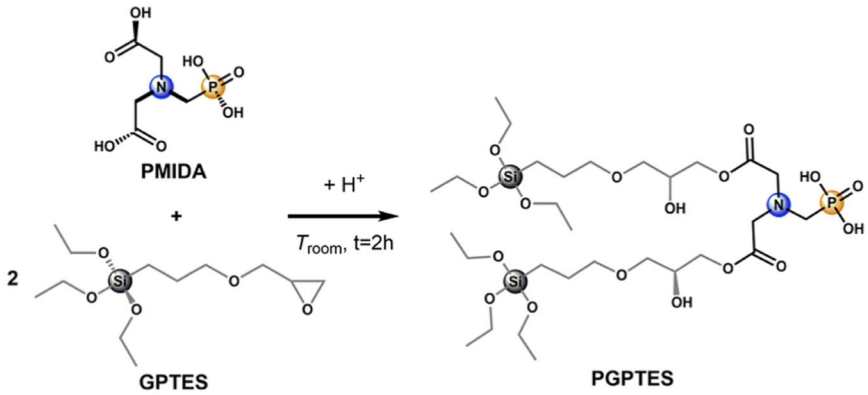

Fig. 15 Scheme of the reaction occurring between PMIDA and GPTES, with the formation of the P-doped precursor PGPTES. Reprinted with permission from ref. [153]. Copyright 2019, Elsevier

	Data	CO_UT	CO_T
Horizontal configuration	t_1 (s)	23	8
	t_2 (s)	76	0
	Total burning time (s)	139	8
	Residue (%)	0	99.5
	FPI (%/s)	0	12.44
	Self-extinction	NO	YES
Vertical configuration	Flammability behaviour		
	Self-extinction	NO	YES

Fig. 16 Flammability behavior and data related to horizontal and vertical flame spread tests for untreated (CO_UT) and sol-gel-treated (CO_T) cotton fabrics. Reprinted with permission from ref. [153]. Copyright 2019, Elsevier

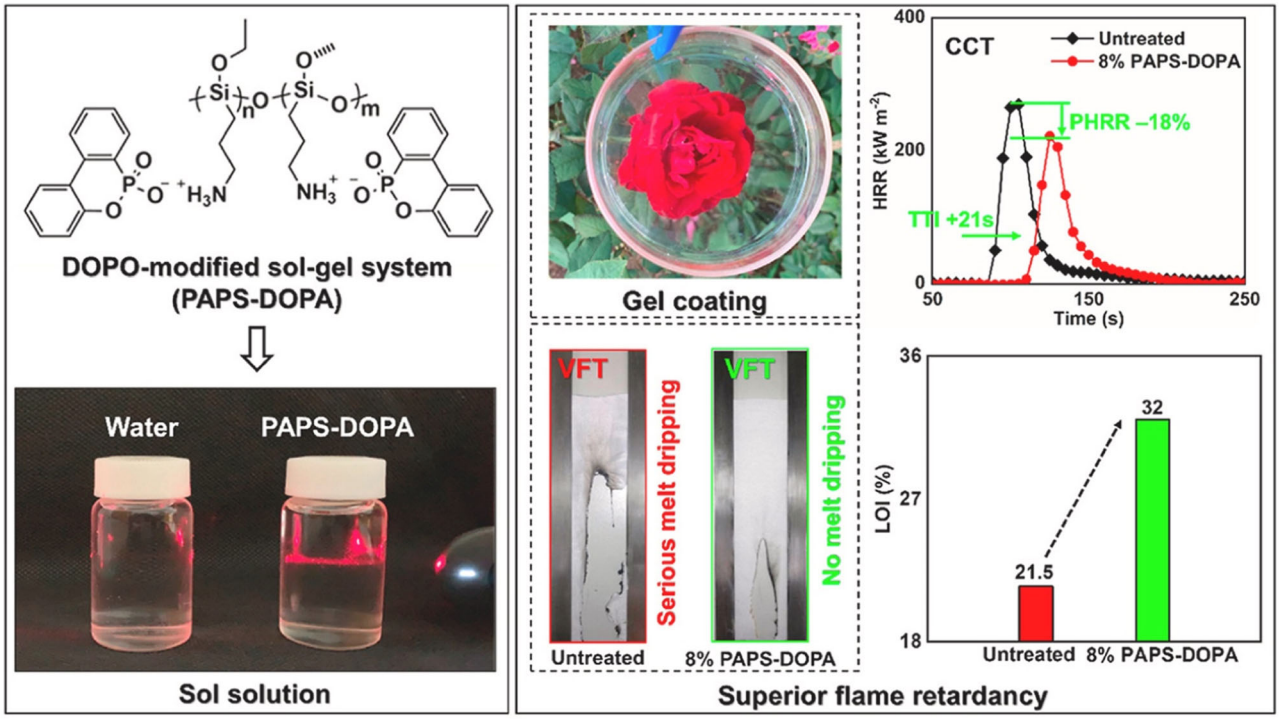

Fig. 17 Structure of 9,10-dihydro-9,10-oxa-10-phosphaphenanthrene-10-oxide (DOPO)-modified colloidal silica (PAPS-DOPA) and flame-retardant behavior of the silk fabrics treated with the designed sol-gel system. Reprinted with permission from ref. [154]. Copyright 2021, Elsevier

self-extinction, hence demonstrating the significant improvement in the fire behavior of the cellulosic substrate.

In addition, as revealed by forced-combustion tests carried out at 35 kW/m^2 irradiative heat flux, the deposited sol-gel-derived coating was responsible for a decrease of both peak of heat released rate and total heat release (by about 12 and 41%, respectively, compared with the untreated fabric), as well as for a remarkable increase of the residue at the end of the tests (1 vs. 26% for untreated and coated fabrics, respectively). These findings were ascribed to the action of the hybrid intumescent coating mainly in the condensed phase, through the formation of a stable and protective char.

Recently, Wang and co-workers [154] investigated the effect of 9,10-dihydro-9,10-oxa-10-phosphaphenanthrene-10-oxide (DOPO)-modified colloidal silica (PAPS-DOPA) obtained by reacting poly(γ-aminopropyl silsesquioxane) (PAPS) with dibenzo[c,e][1,2] oxaphosphinic acid (DOPA). As shown in Fig. 17, the resulting sol–gel coatings deposited on polyester fabrics exhibited high flame retardant features: at 8 wt.% dry add-on, the sol-gel-derived coatings accounted for increased LOI (up to 32.0%, with respect to 21.5% for the untreated fabric), suppression of melt dripping phenomena in vertical flame spread tests, increased time to ignition (TTI), decreased PHRR and total heat release in forced combustion tests (carried out at 35 kW/m^2 irradiative heat flux). The flame-retardant mechanism was ascribed to a predominant gas phase activity due to the presence of the DOPO derivative.

4 Conclusion

Materials based on silicophosphate structures are largely used in various application fields. Nevertheless, for a wider spread of such materials in different technologies, the trade-off between the affinity/instability toward water must be considered, since it plays a key role in their functionality. Therefore, this issue needs to be faced, regardless of the synthesis strategy chosen to obtain these materials. Although the synthesis in inert atmosphere, nonaqueous routes, and the use of suitable solvents represent feasible solutions adopted to overcome this problem, they require strictly controlled reaction conditions, which are energy-demanding and unsuitable for large-scale processes. Conversely, hydrolytic sol-gel routes, if performed in air at room temperature, are a desirable alternative to adopt energy-efficient and eco-friendly protocols. Indeed, they can produce solids with stable Si–O–P linkages, provided that specific stratagems are used, for instance the addition to the binary SiO_2-P_2O_5 system of a third component (X), able to form stable P–O–X and Si–O–X bonding allowing the anchorage of P by the formation of P–O–X–O–Si bridges, or the identification of suitable reaction conditions allowing for the formation of specific micro- or nano-environments, in which phosphorus stabilization can occur. An example of the former approach is the synthesis of ternary oxide systems, with a transition metal such as niobium bridging Si and P in the network. An example of the latter is the in-situ growth of

Si–P phases in a polymer matrix, previously modified by reaction with a suitable coupling agent, accounting for the establishment of a polar micro- or nano-environment in a nonpolar system. Considering the applications of phosphosilicate materials in PEM for fuel cells, solid acid catalysts, flame retardance of composites, coatings, and textiles, it is expected that further research efforts are needed to improve the understanding of the relationship between the synthesis, the functional properties and the stability of the materials. Therefore, the design of new sol-gel strategies may open some significant prospects for advancements in the real-scale applications of these materials.

Author contributions All authors equally contributed to the study conception and design. The first draft of the manuscript was written by CI, AB and AA and all authors commented on the manuscript. All authors read and approved the final manuscript.

Funding Open access funding provided by Università degli Studi di Napoli Federico II within the CRUI-CARE Agreement.

Compliance with ethical standards

Conflict of interest The authors declare no competing interests.

Publisher's note Springer Nature remains neutral with regard to jurisdictional claims in published maps and institutional affiliations.

Abbreviations

APP	ammonium polyphosphate
APTES	(3-aminopropyl)triethoxysilane
CAGR	compound annual growth rate
CMOS	complementary metal-oxide semiconductor
CPB	cetylpyridinium bromide
CTMS	chlorotrimethylsilane
CVD	chemical vapor deposition
DGEBA	bisphenol A diglycidyl ether
DMDCS	dichlorodimethylsilane
DMP	dimethyl ester of H-phosphonic acid
DOPA	dibenzo[c,e][1,2] oxaphosphinic acid
DOPO	9,10-dihydro-9,10-oxa-10-phosphaphenanthrene-10-oxide
DPTS	2-(diethoxyphosphoryl)ethyltriethoxysilane
ED	N,N'-bis[4,6-bis(diethylphosphono)-1,3,5- triazin-yl]-1,2-diaminoethane
EIS	Electrochemical Impedance Spectroscopy
FPS	fibrous phosphosilicate
GPTES	(3-glycidyloxypropyl)triethoxysilane
HA	humic acid
HEMA	hydroxyethyl methacrylate
HPW	phosphotungstic acid
LOI	limiting oxygen index
MPS	(3-methacryloxypropyl)trimethoxysilane
NMR	Nuclear Magnetic Resonance
PA	phytic acid
PAPS	poly(γ-aminopropyl silsesquioxane)
PBI	polybenzimidazole
PDMS	polydimethylsiloxane
PECVD	plasma-enhanced chemical vapor deposition
PEM	proton exchange membrane
PEO	poly(ethylene oxide)
PHRR	peak of heat release rate
PMIDA	N-(phosphonomethyl) iminodiacetic acid
PMMA	poly(methyl methacrylate)
PVA	poly(vinyl alcohol)
RH	relative humidity
SPA	solid phosphoric acid
SPEEK	sulfonated poly(ether ether ketone)
sSEBS	sulfonated styrene-ethylene-butylene-styrene
TEOS	tetraethoxysilane
TEP	triethyl phosphate
TEPI	triethyl phosphite
TMP	trimethyl phosphate
TPD	temperature programmed desorption
TPP	tripolyphosphate
TTI	time to ignition
XPS	X-ray photoelectron spectroscopy
ZSP	zirconium silicophosphate

References

1. Tien T-Y, Hummel FA (1962) The System SiO2-P2O5. J Am Ceram Soc 45:422–424
2. Jiao K, Xuan J, Du Q et al. (2021) Designing the next generation of proton-exchange membrane fuel cells. Nature 595:361–369. https://doi.org/10.1038/s41586-021-03482-7
3. Joseph L, Tumuluri A, Klein LC (2022) Progress in proton conducting sol-gel glasses. J Sol-Gel Sci Technol 102:482–492. https://doi.org/10.1007/s10971-021-05705-9
4. Laberty-Robert C, Vallé K, Pereira F, Sanchez C (2011) Design and properties of functional hybrid organic–inorganic membranes for fuel cells. Chem Soc Rev 40:961–1005. https://doi.org/10.1039/c0cs00144a
5. Busca G, Gervasini A (2020) Solid acids, surface acidity and heterogeneous acid catalysis. Adv Catal 67:1–90. https://doi.org/10.1016/BS.ACAT.2020.09.003
6. Busca G, Ramis G, Lorenzelli V et al. (1989) Phosphoric acid on oxide carriers: 1: characterization of silica, alumina, and titania impregnated by phosphoric Acid. Langmuir 5:911–916. https://doi.org/10.1021/la00088a005
7. Cavani F, Girotti G, Terzoni G (1993) Effect of water in the performance of the "solid phosphoric acid" catalyst for alkylation of benzene to cumene and for oligomerization of propene. Appl Catal A Gen 97:177–196. https://doi.org/10.1016/0926-860X(93)80083-3
8. Hara M, Nakajima K, Kamata K (2015) Recent progress in the development of solid catalysts for biomass conversion into high

value-added chemicals. Sci Technol Adv Mater 16:034903. https://doi.org/10.1088/1468-6996/16/3/034903
9. Deshmukh K, Kovářík T, Křenek T et al. (2020) Recent advances and future perspectives of sol-gel derived porous bioactive glasses: a review. RSC Adv 10:33782–33835. https://doi.org/10.1039/d0ra04287k
10. García A, Izquierdo-Barba I, Colilla M et al. (2011) Preparation of 3-D scaffolds in the SiO2-P2O 5 system with tailored hierarchical meso-macroporosity. Acta Biomater 7:1265–1273. https://doi.org/10.1016/j.actbio.2010.10.006
11. Zagrajczuk B, Dziadek M, Olejniczak Z et al. (2017) Structural and chemical investigation of the gel-derived bioactive materials from the SiO2–CaO and SiO2-CaO-P2O5 systems. Ceram Int 43:12742–12754. https://doi.org/10.1016/J.CERAMINT.2017.06.160
12. Bifulco A, Imparato C, Aronne A, Malucelli G. (2022) Flame retarded polymer systems based on the sol-gel approach: recent advances and future perspectives. J Sol-Gel Sci Technol. https://doi.org/10.1007/s10971-022-05918-6
13. Klingler WW, Bifulco A, Polisi C, et al (2023) Recyclable inherently flame-retardant thermosets: chemistry, properties and applications. Compos Part B Eng 258:110667
14. Malucelli G, Carosio F, Alongi J et al. (2014) Materials engineering for surface-confined flame retardancy. Mater Sci Eng R Rep. 84:1–20. https://doi.org/10.1016/J.MSER.2014.08.001
15. Spontón M, Mercado LA, Ronda JC et al. (2008) Preparation, thermal properties and flame retardancy of phosphorus- and silicon-containing epoxy resins. Polym Degrad Stab 93:2025–2031. https://doi.org/10.1016/J.POLYMDEGRADSTAB.2008.02.014
16. Hsiue G, Liu Y, Tsiao J (2000) Phosphorus-containing epoxy resins for flame retardancy V: synergistic effect of phosphorus–silicon on flame retardancy. J Appl Polym Sci 78:1–7
17. Shang D, Sun X, Hang J et al. (2017) Flame resistance, physical and mechanical properties of UV-cured hybrid coatings containing low-hydroxyl-content sols via an anhydrous sol-gel process. Prog Org Coat 105:267–276. https://doi.org/10.1016/j.porgcoat.2017.01.015
18. Bifulco A, Avolio R, Lehner S et al. (2023) In situ P-Modified Hybrid Silica–Epoxy Nanocomposites via a Green Hydrolytic Sol–Gel route for flame-retardant applications. ACS Appl Nano Mater 6:7422–7435
19. Tian F, Pan L, Wu X, Wu F (1988) The NMR studies of the P2O5-SiO2 sol and gel chemistry. J Non Cryst Solids 104:129–134. https://doi.org/10.1016/0022-3093(88)90191-3
20. Livage J, Barboux P, Vandenborre MT et al. (1992) Sol-gel synthesis of phosphates. J Non Cryst Solids 147–148:18–23. https://doi.org/10.1016/S0022-3093(05)80586-1
21. Szu SP, Klein LC, Greenblatt M (1992) Effect of precursors on the structure of phosphosilicate gels: 29Si and 31 P MAS-NMR study. J Non Cryst Solids 143:21–30. https://doi.org/10.1016/S0022-3093(05)80548-4
22. Fernández-Lorenzo C, Esquivias L, Barboux P et al. (1994) Sol-gel synthesis of SiO2P2O5 glasses. J Non Cryst Solids 176:189–199. https://doi.org/10.1016/0022-3093(94)90077-9
23. Styskalik A, Skoda D, Moravec Z et al. (2014) Synthesis of homogeneous silicophosphate xerogels by non-hydrolytic condensation reactions. Microporous Mesoporous Mater 197:204–212. https://doi.org/10.1016/j.micromeso.2014.06.019
24. Corriu RJP, Leclercq D, Mutin PH et al. (1998) Nonhydrolytic sol-gel routes to layered metal(IV) and silicon phosphonates. J Mater Chem 8:1827–1833. https://doi.org/10.1039/a803755h
25. D'Apuzzo M, Aronne A, Esposito S, Pernice P (2000) Sol-Gel synthesis of humidity-sensitive P2O5-SiO2 amorphous films. J Sol-Gel Sci Technol 17:247–254. https://doi.org/10.1023/A:1008720223563
26. Greenwood NN, Earnshaw A (1997) Chemistry of the elements 2nd Edition. Butterworth-Heinemann, Burlington, MA
27. Boigelot R, Graz Y, Bourgel C et al. (2015) The SiO2-P2O5 binary system: new data concerning the temperature of liquidus and the volatilization of phosphorus. Ceram Int 41:2353–2360. https://doi.org/10.1016/j.ceramint.2014.10.046
28. Bass JD, Grosso D, Boissiere C et al. (2007) Stability of mesoporous oxide and mixed metal oxide materials under biologically relevant conditions. Chem Mater 19:4349–4356. https://doi.org/10.1021/cm071305g
29. García A, Colilla M, Izquierdo-Barba I, Vallet-Regí M (2009) Incorporation of phosphorus into mesostructured silicas: a novel approach to reduce the SiO2 leaching in water. Chem Mater 21:4135–4145. https://doi.org/10.1021/cm9012816
30. Clayden NJ, Esposito S, Pernice P, Aronne A (2001) Solid state 29Si and 31 P NMR study of gel derived phosphosilicate glasses. J Mater Chem 11:936–943. https://doi.org/10.1039/b004107f
31. Coelho C, Babonneau F, Azaïs T et al. (2006) Chemical bonding in silicophosphate gels: contribution of dipolar and J-derived solid state NMR techniques. J Sol-Gel Sci Technol 40:181–189. https://doi.org/10.1007/s10971-006-7431-x
32. Plotnichenko VG, Sokolov VO, Koltashev VV, Dianov EM (2002) On the structure of phosphosilicate glasses. J Non Cryst Solids 306:209–226. https://doi.org/10.1016/S0022-3093(02)01172-9
33. Yadav AK, Singh P (2015) A review of the structures of oxide glasses by Raman spectroscopy. RSC Adv 5:67583–67609. https://doi.org/10.1039/C5RA13043C
34. Massiot P, Centeno MA, Carrizosa I, Odriozola JA (2001) Thermal evolution of sol-gel-obtained phosphosilicate solids (SiPO). J Non Cryst Solids 292:158–166. https://doi.org/10.1016/S0022-3093(01)00854-7
35. Sava BA, Elisa M, Vasiliu IC et al. (2012) Investigations on sol-gel process and structural characterization of SiO 2-P 2 O 5 powders. J Non Cryst Solids 358:2877–2885. https://doi.org/10.1016/j.jnoncrysol.2012.07.016
36. Styskalik A, Skoda D, Moravec Z et al. (2016) Surface reactivity of non-hydrolytic silicophosphate xerogels: a simple method to create Brønsted or Lewis acid sites on porous supports. N. J Chem 40:3705–3715. https://doi.org/10.1039/c5nj02928g
37. Epiphanova A, Magaev O, Vodyankina O (2012) Formation and characterization of phosphate-modified silicate materials derived from sol-gel process. J Sol-Gel Sci Technol 61:509–517. https://doi.org/10.1007/s10971-011-2652-z
38. Takada K, Tamura T, Kasuga T (2022) Structure and dissolution of silicophosphate glass. RSC Adv 12:34882–34889. https://doi.org/10.1039/d2ra06707b
39. Stotskaya OA, Poddenezhnyi EN, Boiko AA et al. (2008) Dehydroxylation of sol-gel glasses and glass composites with the use of aerosils modified by phosphorus compounds. Glass Phys Chem 34:569–574. https://doi.org/10.1134/S1087659608050076
40. Todan L, Anghel EM, Osiceanu P et al. (2015) Structural characterization of some sol-gel derived phosphosilicate glasses. J Mol Struct 1086:161–171. https://doi.org/10.1016/j.molstruc.2015.01.012
41. Anastasescu M, Gartner M, Ghita A et al. (2006) Loss of phosphorous in silica-phosphate sol-gel films. J Sol-Gel Sci Technol 40:325–333. https://doi.org/10.1007/s10971-006-8775-y
42. Samba-Fouala C, Mossoyan JC, Mossoyan-Déneux M et al. (2000) Preparation and properties of silica hybrid gels containing phytic acid. J Mater Chem 10:387–393. https://doi.org/10.1039/a908289a
43. Qiu D, Guerry P, Knowles JC et al. (2008) Formation of functional phosphosilicate gels from phytic acid and tetraethyl orthosilicate. J Sol-Gel Sci Technol 48:378–383. https://doi.org/10.1007/s10971-008-1818-9

44. Pathania D, Sharma G, Thakur R (2015) Pectin @ zirconium (IV) silicophosphate nanocomposite ion exchanger: photo catalysis, heavy metal separation and antibacterial activity. Chem Eng J 267:235–244. https://doi.org/10.1016/j.cej.2015.01.004
45. Wang Y, Wang H, Meng X, Chen R (2014) Antireflective films with Si–O–P linkages from aqueous colloidal silica: preparation, formation mechanism and property. Sol Energy Mater Sol Cells 130:71–82. https://doi.org/10.1016/J.SOLMAT.2014.06.040
46. Khabbouchi M, Hosni K, Mezni M, Srasra E (2018) Simplified synthesis of silicophosphate materials using an activated metakaolin as a natural source of active silica. Appl Clay Sci 158:169–176. https://doi.org/10.1016/J.CLAY.2018.03.027
47. Borni M, Hajji M, Hamzaoui AH, Triki M (2022) Synthesis and characterization of silicophosphates using phosphoric acid and silica gel prepared from tunisian sand. Silicon 14:8939–8948. https://doi.org/10.1007/S12633-021-01602-6/METRICS
48. Wang L, Samuels WD, Exarhos GJ et al. (1998) 31 P and 29 Si NMR study of sol–gel-synthesized phosphate ceramics. J Mater Chem 8:165–169
49. Aronne A, Turco M, Bagnasco G et al. (2005) Synthesis of high surface area phosphosilicate glasses by a modified Sol−Gel Method. Chem Mater 17:2081–2090. https://doi.org/10.1021/cm047768t
50. Clayden NJ, Accardo G, Mazzei P et al. (2015) Phosphorus stably bonded to a silica gel matrix through niobium bridges. J Mater Chem A 3:15986–15995. https://doi.org/10.1039/C5TA03267A
51. Clayden NJ, Imparato C, Avolio R et al. (2020) Chloride-free hydrolytic sol-gel synthesis of Nb-P-Si oxides: an approach to solid acid materials. Green Chem 22:7140–7151. https://doi.org/10.1039/d0gc02519d
52. Miyabe D, Takahashi M, Tokuda Y et al. (2005) Structure and formation mechanism of six-fold coordinated silicon in phosphosilicate glasses. Phys Rev B - Condens Matter Mater Phys 71:172202. https://doi.org/10.1103/PHYSREVB.71.172202/FIGURES/3/MEDIUM
53. Ren J, Eckert H (2018) Superstructural units involving six-coordinated silicon in sodium phosphosilicate glasses detected by solid-state nmr spectroscopy. J Phys Chem C 122:27620–27630. https://doi.org/10.1021/acs.jpcc.8b09779
54. Zeng H, Jiang Q, Li X et al. (2015) Anneal-induced enhancement of refractive index and hardness of silicophosphate glasses containing six-fold coordinated silicon. Appl Phys Lett 106:21903. https://doi.org/10.1063/1.4905839/29742
55. Omata T, Sharma A, Suzuki I, et al. (2022) Anhydrous silicophosphoric acid glass: thermal properties and proton conductivity. ChemPhysChem 23: https://doi.org/10.1002/cphc.202100840
56. Sinkó K, Meiszterics A, Rohonczy J et al. (2017) Effect of phosphorus precursors on the structure of bioactive calcium phosphate silicate systems. Mater Sci Eng C 73:767–777. https://doi.org/10.1016/j.msec.2016.12.130
57. Wong CY, Wong WY, Ramya K et al. (2019) Additives in proton exchange membranes for low- and high-temperature fuel cell applications: A review. Int J Hydrog Energy 44:6116–6135. https://doi.org/10.1016/j.ijhydene.2019.01.084
58. Nogami M, Nagao R, Wong C et al. (1999) High proton conductivity in porous P2O5−SiO2 Glasses. J Phys Chem B 103:9468–9472. https://doi.org/10.1021/jp991277s
59. Nogami M, Matsushita H, Goto Y, Kasuga T (2000) A sol-gel-derived glass as a fuel cell electrolyte. Adv Mater 12:1370–1372
60. Nogami M, Daiko Y, Akai T, Kasuga T (2001) Dynamics of proton transfer in the sol−gel-derived P 2 O 5 −SiO 2 Glasses. J Phys Chem B 105:4653–4656. https://doi.org/10.1021/jp010611t
61. Nogami M, Daiko Y, Goto Y et al. (2003) Sol-gel preparation of fast proton-conducting P2O5-SiO2 glasses. J Sol-Gel Sci Technol 26:1041–1044. https://doi.org/10.1023/A:1020738219538
62. Daiko Y, Kasuga T, Nogami M (2004) Pore size effect on proton transfer in sol-gel porous silica glasses. Microporous Mesoporous Mater 69:149–155. https://doi.org/10.1016/j.micromeso.2004.02.005
63. Clayden NJ, Esposito S, Aronne A (2001) Chemical heterogeneity in phosphosilicate gels by NMR magnetisation exchange. J Chem Soc Dalt Trans 13:2003–2008. https://doi.org/10.1039/b100474n
64. Esposito S, Clayden NJ, Cottrell SP (2020) Muon spin relaxation study of phosphosilicate gels. Solid State Ion 348:115287. https://doi.org/10.1016/j.ssi.2020.115287
65. Daiko Y (2014) Proton conduction in nanopores of sol-gel-derived porous glasses and thin films. J Sol-Gel Sci Technol 70:172–179. https://doi.org/10.1007/s10971-014-3297-5
66. Matsuda A, Kanzaki T, Tadanaga K et al. (2001) Medium temperature range characterization as a proton conductor for phosphosilicate dry gels containing large amounts of phosphorus. Electrochim Acta 47:939–944. https://doi.org/10.1016/S0013-4686(01)00810-6
67. Matsuda A, Kanzaki T, Tatsumisago M, Minami T (2001) Comparison of structure and proton conductivity of phosphosilicate gels derived from several kinds of phosphorus-containing compounds. Solid State Ion 145:161–166. https://doi.org/10.1016/S0167-2738(01)00945-6
68. Tung SP, Hwang BJ (2005) Synthesis and characterization of hydrated phosphor-silicate glass membrane prepared by an accelerated sol-gel process with water/rapor management. J Mater Chem 15:3532–3538. https://doi.org/10.1039/b505918f
69. Xiong L, Shi J, Zhang L, Nogami M (2007) Facile one-step synthesis of highly ordered bimodal mesoporous phosphosilicate monoliths. J Am Chem Soc 129:11878–11879. https://doi.org/10.1021/JA070466I/SUPPL_FILE/JA070466ISI20070829_012605.PDF
70. Li H, Jin D, Kong X et al. (2011) High proton-conducting monolithic phosphosilicate glass membranes. Microporous Mesoporous Mater 138:63–67. https://doi.org/10.1016/J.MICROMESO.2010.09.029
71. Aparicio M, Damay F, Klein LC (2003) Characterization of SiO 2-P 2 O 5-ZrO 2 Sol-Gel/NAFION TM Composite Membranes. J Sol-Gel Sci Technol 26:1055–1059
72. Mosa J, Larramona G, Durán A, Aparicio M (2008) Synthesis and characterization of P2O5–ZrO2–SiO2 membranes doped with tungstophosphoric acid (PWA) for applications in PEMFC. J Memb Sci 307:21–27. https://doi.org/10.1016/j.memsci.2007.06.035
73. Uma T, Izuhara S, Nogami M (2006) Structural and proton conductivity study of P2O5-TiO2-SiO2 glasses. J Eur Ceram Soc 26:2365–2372. https://doi.org/10.1016/J.JEURCERAMSOC.2005.04.013
74. Mroczkowska-Szerszeń M, Siekierski M, Letmanowski R et al. (2013) Synthetic preparation of proton conducting polyvinyl alcohol and TiO2-doped inorganic glasses for hydrogen fuel cell applications. Electrochim Acta 104:487–495. https://doi.org/10.1016/j.electacta.2013.01.005
75. Zhou Y, Yang J, Su H et al. (2014) Insight into proton transfer in phosphotungstic acid functionalized mesoporous silica-based proton exchange membrane fuel cells. J Am Chem Soc 136:4954–4964. https://doi.org/10.1021/JA411268Q/SUPPL_FILE/JA411268Q_SI_001.PDF
76. Aricò AS, Baglio V, Di Blasi A et al. (2003) Influence of the acid–base characteristics of inorganic fillers on the high temperature performance of composite membranes in direct methanol fuel cells. Solid State Ion 161:251–265. https://doi.org/10.1016/S0167-2738(03)00283-2
77. Sun X, Simonsen SC, Norby T, Chatzitakis A (2019) Composite membranes for high temperature PEM fuel cells and

electrolysers: a critical review. Membranes (Basel) 9: https://doi.org/10.3390/membranes9070083
78. Dhanapal D, Xiao M, Wang S, Meng Y (2019) A review on sulfonated polymer composite/organic-inorganic hybrid membranes to address methanol barrier issue for methanol fuel cells Nanomater 9:668. https://doi.org/10.3390/NANO9050668
79. Jiang F, Di Z, Li H et al. (2011) Fast proton-conducting glass membrane based on porous phosphosilicate and perfluorosulfonic acid polymer. J Power Sources 196:1048–1054. https://doi.org/10.1016/J.JPOWSOUR.2010.08.030
80. Mistry MK, Choudhury NR, Dutta NK et al. (2008) Novel organic - Inorganic hybrids with increased water retention for elevated temperature proton exchange membrane application. Chem Mater 20:6857–6870. https://doi.org/10.1021/CM801374H/ASSET/IMAGES/MEDIUM/CM-2008-01374H_0012.GIF
81. Lakshminarayana G, Nogami M, Kityk IV (2010) Synthesis and characterization of anhydrous proton conducting inorganic–organic composite membranes for medium temperature proton exchange membrane fuel cells (PEMFCs). Energy 35:5260–5268. https://doi.org/10.1016/J.ENERGY.2010.07.039
82. Kannan AG, Choudhury NR, Dutta NK (2007) Synthesis and characterization of methacrylate phospho-silicate hybrid for thin film applications. Polym (Guildf) 48:7078–7086. https://doi.org/10.1016/j.polymer.2007.09.050
83. Xie Q, Li Y, Chen X et al. (2015) Composite proton exchange membranes based on phosphosilicate sol and sulfonated poly(-ether ether ketone) for fuel cell applications. J Power Sources 282:489–497. https://doi.org/10.1016/j.jpowsour.2015.02.037
84. Chen X, Zhang Y, Li M et al. (2017) A flexible phosphosilicate-based intermediate temperature composite electrolyte membrane with proton conductivity at temperatures of up to 250 °C. Int J Hydrog Energy 42:28829–28835. https://doi.org/10.1016/j.ijhydene.2017.10.005
85. Zhang J, Aili D, Bradley J et al. (2017) In situ formed phosphoric acid/phosphosilicate nanoclusters in the exceptional enhancement of durability of polybenzimidazole membrane fuel cells at elevated high temperatures. J Electrochem Soc 164:F1615–F1625. https://doi.org/10.1149/2.1051714jes
86. Castro Y, Mosa J, Aparicio M et al. (2015) Sol–gel hybrid membranes loaded with meso/macroporous SiO2, TiO2–P2O5 and SiO2–TiO2–P2O5 materials with high proton conductivity. Mater Chem Phys 149–150:686–694. https://doi.org/10.1016/J.MATCHEMPHYS.2014.11.028
87. Chen B, Li G, Wang L et al. (2013) Proton conductivity and fuel cell performance of organic–inorganic hybrid membrane based on poly(methyl methacrylate)/silica. Int J Hydrog Energy 38:7913–7923. https://doi.org/10.1016/J.IJHYDENE.2013.03.167
88. Santiago Ó, Mosa J, Escribano PG et al. (2020) 40SiO2–40P2O5–20ZrO2 sol-gel infiltrated sSEBS membranes with improved methanol crossover and cell performance for direct methanol fuel cell applications. Int J Hydrog Energy 45:20620–20631. https://doi.org/10.1016/J.IJHYDENE.2020.01.252
89. Siekierski M, Mroczkowska-Szerszeń M, Letmanowski R, et al (2020) Ionic transport properties of P2O5-SiO2 glassy protonic composites doped with polymer and inorganic titanium-based fillers. Materials (Basel) 13: https://doi.org/10.3390/ma13133004
90. Sukhyy KM, Gomza YP, Belyanovskaya EA et al. (2015) Resistive humidity sensors based on proton-conducting organic–inorganic silicophosphates doped by polyionenes. J Sol-Gel Sci Technol 74:472–481. https://doi.org/10.1007/S10971-015-3622-7/METRICS
91. Onen M, Emond N, Li J et al. (2021) CMOS-compatible protonic programmable resistor based on phosphosilicate glass electrolyte for analog deep learning. Nano Lett 21:6111–6116. https://doi.org/10.1021/acs.nanolett.1c01614
92. Kamal M, Battisha IK, Salem MA, El Nahrawy AMS (2011) Structural and thermal properties of monolithic silica-phosphate (SiO 2-P2O5) gel glasses prepared by sol-gel technique. J Sol-Gel Sci Technol 58:507–517. https://doi.org/10.1007/s10971-011-2420-0
93. Amin A, Ahmed EH, Wickleder C et al. (2019) Phosphosilicate–polyamidoamine hyperbranched polymer–Er3+ nanocomposite toward planar optical waveguide applications. Polym Compos 40:2029–2038. https://doi.org/10.1002/PC.24984
94. Di X, Hu Z, Jiang J et al. (2017) Use of long-term stable CsPbBr3 perovskite quantum dots in phospho-silicate glass for highly efficient white LEDs. Chem Commun 53:11068–11071. https://doi.org/10.1039/C7CC06486A
95. Chen D, Yuan S, Chen X et al. (2018) CsPbX3 (X = Br, I) perovskite quantum dot embedded low-melting phosphosilicate glasses: controllable crystallization, thermal stability and tunable emissions. J Mater Chem C 6:6832–6839. https://doi.org/10.1039/C8TC02407C
96. Di Francesca D, Vecchi GL, Girard S et al. (2019) Qualification and calibration of single-mode phosphosilicate optical fiber for dosimetry at CERN. J Light Technol 37:4643–4649. https://doi.org/10.1109/JLT.2019.2915510
97. Coetzee JH, Mashapa TN, Prinsloo NM, Rademan JD (2006) An improved solid phosphoric acid catalyst for alkene oligomerization in a Fischer-Tropsch refinery. Appl Catal A Gen 308:204–209. https://doi.org/10.1016/j.apcata.2006.04.023
98. Zhang J, Yan Y, Chu Q, Feng J (2015) Solid phosphoric acid catalyst for propene oligomerization: effect of silicon phosphate composition. Fuel Process Technol 135:2–5. https://doi.org/10.1016/J.FUPROC.2014.09.007
99. Santander JA, Alvarez M, Gutierrez V, Volpe MA (2019) Solid phosphoric acid catalysts based on mesoporous silica for levoglucosenone production via cellulose fast pyrolysis. J Chem Technol Biotechnol 94:484–493. https://doi.org/10.1002/JCTB.5795
100. Zhang G, Yang C, Miller JT et al. (2018) Tetrahedral Nickel(II) Phosphosilicate Single-Site Selective Propane Dehydrogenation Catalyst. ChemCatChem 10:961–964. https://doi.org/10.1002/CCTC.201701815
101. Jain SK, Tabassum T, Li L et al. (2021) P-site structural diversity and evolution in a zeosil catalyst. J Am Chem Soc 143:1968–1983. https://doi.org/10.1021/JACS.0C11768/SUPPL_FILE/JA0C11768_SI_001.PDF
102. Cho HJ, Ren L, Vattipalli V et al. (2017) Renewable p-Xylene from 2,5-Dimethylfuran and Ethylene Using Phosphorus-Containing Zeolite Catalysts. ChemCatChem 9:398–402. https://doi.org/10.1002/CCTC.201601294
103. Zhiani R, Khoobi M, Sadeghzadeh SM (2019) Phosphosilicate nanosheets for supported palladium nanoparticles as a novel nanocatalyst. Microporous Mesoporous Mater 275:76–86. https://doi.org/10.1016/j.micromeso.2018.08.021
104. Yu L, Xing S, Zheng K (2021) The Synthesis of Cyclic Carbonates from Oxidative Carboxylation Under Mild Conditions Using Al/FPS Nanocatalyst. Catal Lett 151:600–611. https://doi.org/10.1007/S10562-020-03315-8/FIGURES/14
105. Zhiani R, Khoobi M, Sadeghzadeh SM (2020) Ruthenium–birhodanine complex supported over fibrousphosphosilicate for photocatalytic CO2 reduction to formate. Catal Today 340:197–203. https://doi.org/10.1016/J.CATTOD.2018.09.034
106. Ganesan K, Hayagreevan C, Rahul R et al. (2023) Catalytic hydrolysis of sodium borohydride for hydrogen production using phosphorylated silica particles. Environ Sci Pollut Res 30:21199–21212. https://doi.org/10.1007/S11356-022-23672-8/METRICS

107. Styskalik A, Skoda D, Moravec Z et al. (2015) Control of micro/mesoporosity in non-hydrolytic hybrid silicophosphate xerogels. J Mater Chem A 3:7477–7487. https://doi.org/10.1039/C4TA06823H
108. Mohd Ekhsan J, Lee SL, Nur H (2014) Niobium oxide and phosphoric acid impregnated silica-titania as oxidative-acidic bifunctional catalyst. Appl Catal A Gen 471:142–148. https://doi.org/10.1016/j.apcata.2013.11.041
109. García-Sancho C, Cecilia JA, Mérida-Robles JM et al. (2018) Effect of the treatment with H3PO4 on the catalytic activity of Nb2O5 supported on Zr-doped mesoporous silica catalyst. Case study: Glycerol dehydration. Appl Catal B Environ 221:158–168. https://doi.org/10.1016/j.apcatb.2017.09.016
110. Paul M, Pal N, Ali M, Bhaumik A (2010) New mesoporous silicotitaniumphosphate and its application in acid catalysis and adsorption of As(III/V), Cd(II) and Hg(II). J Mol Catal A Chem 330:49–55. https://doi.org/10.1016/J.MOLCATA.2010.07.001
111. Aronne A, Di Serio M, Vitiello R et al. (2017) An environmentally Friendly Nb-P-Si solid catalyst for acid-demanding reactions. J Phys Chem C 121:17378–17389. https://doi.org/10.1021/acs.jpcc.7b05886
112. Gervasini A, Carniti P, Bossola F et al. (2018) New Nb-P-Si ternary oxide materials and their use in heterogeneous acid catalysis. Mol Catal 458:280–286. https://doi.org/10.1016/j.mcat.2017.10.006
113. Gervasini A, Campisi S, Carniti P et al. (2019) Influence of the Nb/P ratio of acidic Nb-P-Si oxides on surface and catalytic properties. Appl Catal A Gen 579:9–17. https://doi.org/10.1016/j.apcata.2019.04.008
114. Garbarino G, Pampararo G, Finocchio E et al. (2022) Surface acid properties of Nb2O5–P2O5–SiO2 gel-derived catalysts. Microporous Mesoporous Mater 343:112190. https://doi.org/10.1016/j.micromeso.2022.112190
115. Currell BR, Frazer MJ (1969) Inorganic polymers. R Inst Chem Rev 2:13–40
116. Xu J, Hadjichristidis N (2023) Heteroatom-containing degradable polymers by ring-opening metathesis polymerization. Prog Polym Sci 101656
117. Zhu S, Gong W, Luo J et al. (2019) Flame retardancy and mechanism of novel phosphorus-silicon flame retardant based on polysilsesquioxane. Polym (Basel) 11:1304
118. Ullah RS, Wang L, Yu H et al. (2017) Synthesis of polyphosphazenes with different side groups and various tactics for drug delivery. RSC Adv 7:23363–23391
119. Brook MA, Grande JB, Ganachaud F (2011) New synthetic strategies for structured silicones using B (C 6F 5) 3. Silicon Polym 161–183
120. Yu D, Kleemeier M, Wu GM et al. (2011) Phosphorus and silicon containing low-melting organic–inorganic glasses improve flame retardancy of epoxy/clay composites. Macromol Mater Eng 296:952–964
121. Priegert AM, Rawe BW, Serin SC, Gates DP (2016) Polymers and the p-block elements. Chem Soc Rev 45:922–953
122. Borisov SN, Voronkov MG, Lukevits EY, et al (1971) Organosilicon Derivatives of Phosphorus. Organosilicon Deriv Phosphorus Sulfur 1–155
123. Rabinowitz R (1963) The reactions of phosphonic acid esters with acid chlorides. A very mild hydrolytic route. J Org Chem 28:2975–2978
124. Troev K, Delimarinova U, Shenkov S (1993) Synthesis of phosphorus-, silicon-and chlorine-containing oligomers. Eur Polym J 29:613–616
125. Derouet D, Cauret L, Brosse J-C (2004) Synthesis of poly (silylenephosphonate) s incorporating 2-chloroethylphosphonic acid (ethephon), a stimulant for the latex production by the Hevea brasiliensis. Eur Polym J 40:1953–1966
126. Mitova V, Shestakova P, Koseva N, Troev K (2019) Phosphorus and silicon containing inorganic polymer Poly (dimethylsilane H-phosphonate): synthesis and NMR Spectroscopic Characterization. Eur J Inorg Chem 2019:1679–1687
127. Liu L, Zhang W, Yang R (2020) Flame retardant epoxy composites with epoxy-containing polyhedral oligomeric silsesquioxanes. Polym Adv Technol 31:2058–2074
128. Ye X, Li J, Zhang W et al. (2020) Fabrication of eco-friendly and multifunctional sodium-containing polyhedral oligomeric silsesquioxane and its flame retardancy on epoxy resin. Compos Part B Eng 191:107961
129. Bifulco A, Tescione F, Capasso A et al. (2018) Effects of post cure treatment in the glass transformation range on the structure and fire behavior of in situ generated silica/epoxy hybrids. J Sol-Gel Sci Technol 87:156–169. https://doi.org/10.1007/s10971-018-4710-2
130. Bifulco A, Parida D, Salmeia KA et al. (2020) Fire and mechanical properties of DGEBA-based epoxy resin cured with a cycloaliphatic hardener: combined action of silica, melamine and DOPO-derivative. Mater Des 193:108862
131. Wang K, Liu H, Wang C et al. (2020) Flame-retardant performance of epoxy resin composites with SiO2 nanoparticles and phenethyl-bridged DOPO derivative. ACS omega 6:666–674
132. Guadagno L, Raimondo M, Vittoria V et al. (2014) Development of epoxy mixtures for application in aeronautics and aerospace. Rsc Adv 4:15474–15488
133. Moreira VB, Alemán C, Rintjema J et al. (2022) A biosourced epoxy resin for adhesive thermoset applications. ChemSusChem 15:e202102624
134. Post W, Susa A, Blaauw R et al. (2020) A review on the potential and limitations of recyclable thermosets for structural applications. Polym Rev 60:359–388
135. Memon H, Wei Y, Zhu C (2022) Recyclable and reformable epoxy resins based on dynamic covalent bonds–Present, past, and future. Polym Test 105:107420
136. Zhi M, Yang X, Fan R, et al (2022) A comprehensive review of reactive flame-retardant epoxy resin: fundamentals, recent developments, and perspectives. Polym Degrad Stab 109976
137. Bifulco A, Varganici C, Rosu L, et al (2022) Recent advances in flame retardant epoxy systems containing non-reactive DOPO based phosphorus additives. Polym Degrad Stab 109962
138. Özmen FK, Üreyen ME, Koparal AS (2020) Cleaner production of flame-retardant-glass reinforced epoxy resin composite for aviation and reducing smoke toxicity. J Clean Prod 276:124065
139. Varganici C-D, Rosu L, Bifulco A, et al (2022) Recent advances in flame retardant epoxy systems from reactive DOPO–based phosphorus additives. Polym Degrad Stab 202:110020
140. Branda F, Bifulco A, Jehnichen D et al. (2021) Structure and bottom-up formation mechanism of multisheet silica-based nanoparticles formed in an epoxy matrix through an in situ process. Langmuir 37:8886–8893
141. Bifulco A, Parida D, Salmeia KA et al. (2020) Improving flame retardancy of in-situ silica-epoxy nanocomposites cured with aliphatic hardener: combined effect of DOPO-based flame-retardant and melamine. Compos Part C Open Access 2:100022
142. Venezia V, Matta S, Lehner S et al. (2021) Detailed thermal, fire, and mechanical study of silicon-modified epoxy resin containing humic acid and other additives. ACS Appl Polym Mater 3:5969–5981
143. Chiang C-L, Chang R-C (2008) Synthesis, characterization and properties of novel self-extinguishing organic–inorganic nanocomposites containing nitrogen, silicon and phosphorus via sol–gel method. Compos Sci Technol 68:2849–2857
144. Chiang C-L, Ma C-CM (2002) Synthesis, characterization and thermal properties of novel epoxy containing silicon and phosphorus nanocomposites by sol–gel method. Eur Polym J 38:2219–2224

145. Parida D, Salmeia KA, Sadeghpour A et al. (2021) Template-free synthesis of hybrid silica nanoparticle with functionalized mesostructure for efficient methylene blue removal. Mater Des 201:109494. https://doi.org/10.1016/j.matdes.2021.109494
146. Alongi J, Malucelli G (2012) State of the art and perspectives on sol–gel derived hybrid architectures for flame retardancy of textiles. J Mater Chem 22:21805–21809. https://doi.org/10.1039/C2JM32513F
147. Malucelli G (2020) Sol-Gel and layer-by-layer coatings for flame-retardant cotton fabrics: recent advances Coatings 10:333. https://doi.org/10.3390/COATINGS10040333
148. Brancatelli G, Colleoni C, Massafra MR, Rosace G (2011) Effect of hybrid phosphorus-doped silica thin films produced by sol-gel method on the thermal behavior of cotton fabrics. Polym Degrad Stab 96:483–490. https://doi.org/10.1016/J.POLYMDEGRADSTAB.2011.01.013
149. Alongi J, Ciobanu M, Malucelli G (2011) Novel flame retardant finishing systems for cotton fabrics based on phosphorus-containing compounds and silica derived from sol–gel processes. Carbohydr Polym 85:599–608. https://doi.org/10.1016/J.CARBPOL.2011.03.024
150. Cheng XW, Liang CX, Guan JP et al. (2018) Flame retardant and hydrophobic properties of novel sol-gel derived phytic acid/silica hybrid organic-inorganic coatings for silk fabric. Appl Surf Sci 427:69–80. https://doi.org/10.1016/J.APSUSC.2017.08.021
151. Cireli A, Onar N, Ebeoglugil MF et al. (2007) Development of flame retardancy properties of new halogen-free phosphorous doped SiO2 thin films on fabrics. J Appl Polym Sci 105:3748–3756. https://doi.org/10.1002/APP.26442
152. Yaman N (2009) Preparation and flammability properties of hybrid materials containing phosphorous compounds via sol-gel process. Fibers Polym 10:413–418. https://doi.org/10.1007/S12221-009-0413-1/METRICS
153. Castellano A, Colleoni C, Iacono G et al. (2019) Synthesis and characterization of a phosphorous/nitrogen based sol-gel coating as a novel halogen- and formaldehyde-free flame retardant finishing for cotton fabric. Polym Degrad Stab 162:148–159. https://doi.org/10.1016/J.POLYMDEGRADSTAB.2019.02.006
154. Wang QZ, Liu C, Xu YJ et al. (2021) Highly efficient flame retardation of polyester fabrics via novel DOPO-modified sol-gel coatings. Polym (Guildf) 226:123761. https://doi.org/10.1016/J.POLYMER.2021.123761
155. Fărcaş AC, Dobra P (2014) Adaptive control of membrane conductivity of PEM fuel cell. Procedia Technol 12:42–49. https://doi.org/10.1016/J.PROTCY.2013.12.454
156. National Center for Biotechnology Information (2023). Periodic Table of Elements. Retrieved April 30, 2023 from https://pubchem.ncbi.nlm.nih.gov/periodic-table/